Supporting Information

Asymmetric Heteroleptic Ir(III) Phosphorescent Complexes with Aromatic Selenide and Selenophene Groups: Synthesis and Photophysical, Electrochemical, and Electrophosphorescent Behaviors

Zhao Feng,[†] Dezhi Wang,[‡] Xiaolong Yang,[†] Deyuan Jin,[†] Daokun Zhong,[†] Boao Liu,[†] Guijiang Zhou,*[,†] Miaofeng Ma*[,‡] and Zhaoxin Wu*[,¶]

[†]MOE Key Laboratory for Nonequilibrium Synthesis and Modulation of Condensed Matter, Institute of Chemistry for New Energy Materials, Department of Chemistry, School of Science, Xi'an Jiaotong University, Xi'an 710049, People's Republic of China

[‡] Department of Applied Chemistry, College of Chemistry & Pharmacy, Northwest A&F University, Yangling 712100, People's Republic of China

[¶]Key Laboratory of Photonics Technology for Information School of Electronic and Information Engineering, Xi'an Jiaotong University, Xi'an 710049, People's Republic of China

*Guijiang Zhou: E-mail, zhougj@mail.xjtu.edu.cn

*Miaofeng Ma: E-mail, mmfyangling@126.com

*Zhaoxin Wu: E-mail, zhaoxinwu@mail.xjtu.edu.cn

Contents

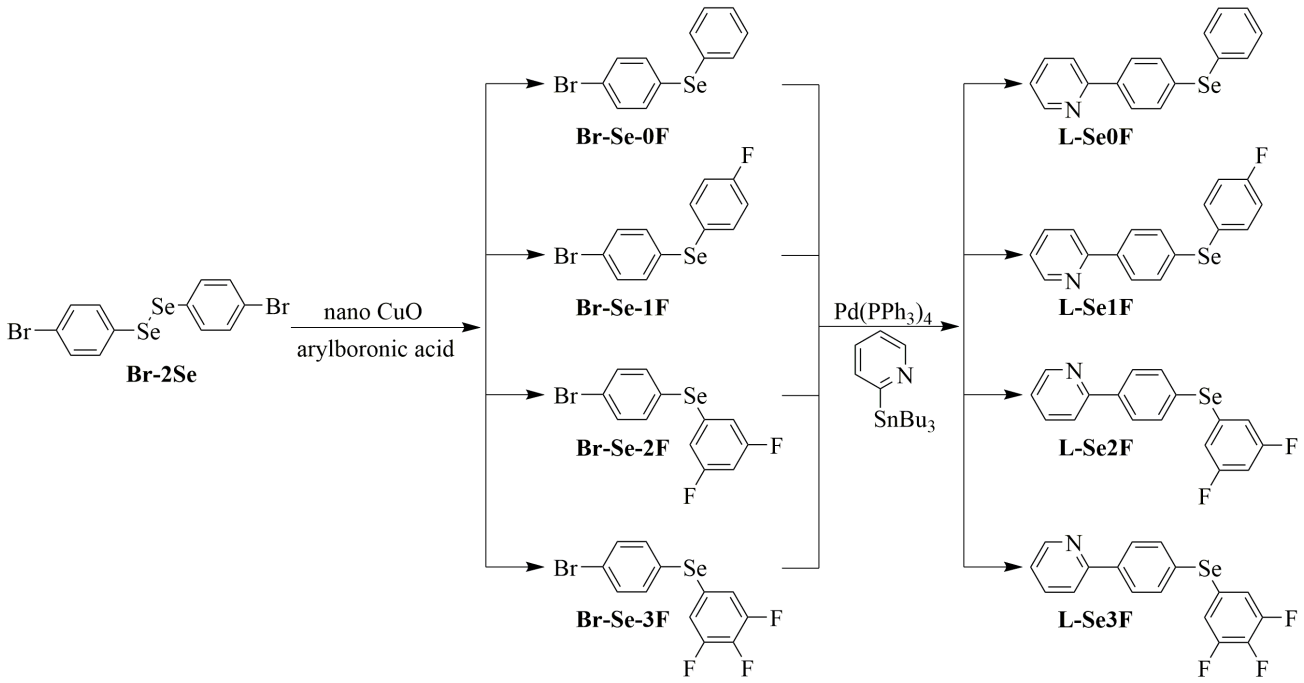

Scheme S1. Synthesis of the organic ligands through selenide intermediate compounds.

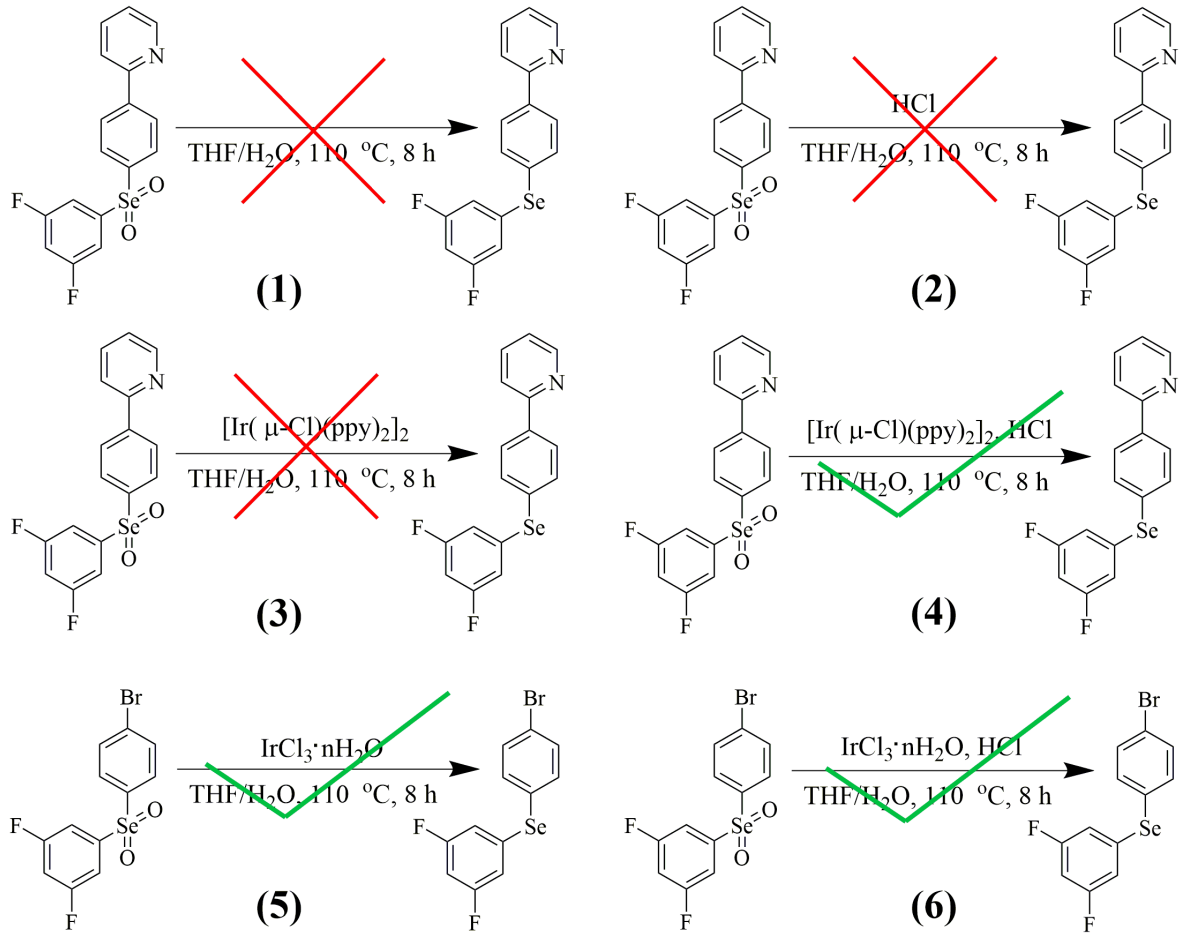

Scheme S2. Experimental investigation of the selenone group (–SeO_2Ar) reduction.

Table S1. The reaction results of the selenone group (–SeO_2Ar) reduction experiments.

Reaction Entry	Starting Material	Reaction Conditions [a]	Yield
1	L-SeO-2F	THF/H_2O (3:1, v/v), 110 ^oC, 8 h.	- [b]
2	L-SeO-2F	THF/H_2O (3:1, v/v), HCl, 110 ^oC, 8 h.	-
3	L-SeO-2F	THF/H_2O (3:1, v/v), $[Ir(\mu\text{-}Cl)(ppy)_2]_2$, 110 ^oC, 8 h.	-
4	L-SeO-2F	THF/H_2O (3:1, v/v), $[Ir(\mu\text{-}Cl)(ppy)_2]_2$, HCl, 110 ^oC, 8 h.	45%
5	Br-SeO-2F	THF/H_2O (3:1, v/v), $IrCl_3{\cdot}nH_2O$, 110 ^oC, 8 h.	95%
6	Br-SeO-2F	THF/H_2O (3:1, v/v), $IrCl_3{\cdot}nH_2O$, HCl, 110 ^oC, 8 h.	96%

[a] In all the reactions, the molar ratio between the starting material and Ir(III) containing compound was *ca.* 1:1. [b] Cannot be detected properly.

Table S2. Selected structural parameters of **IrSe-2F**.

Bond angles (°)				Bond lengths (Å)	
C(7)-Ir(1)-C(24)	91.7 (3)	C(7)-Ir(1)-N(1)	80.8 (3)	Ir(1)-C(7)	2.004 (7)
C(24)-Ir(1)-N(1)	94.7 (3)	C(7)-Ir(1)-N(2)	96.6 (3)	Ir(1)-C(24)	2.006 (6)
C(24)-Ir(1)-N(2)	80.3 (3)	N(1)-Ir(1)-N(2)	174.3 (3)	Ir(1)-N(1)	2.027 (7)
C(7)-Ir(1)-O(2)	174.9 (3)	C(24)-Ir(1)-O(2)	88.8 (3)	Ir(1)-N(2)	2.045 (5)
N(1)-Ir(1)-O(2)	94.1 (3)	N(2)-Ir(1)-O(2)	88.5 (2)	Ir(1)-O(2)	2.134 (5)
C(7)-Ir(1)-O(1)	91.5 (2)	C(24)-Ir(1)-O(1)	173.2 (3)	Ir(1)-O(1)	2.139 (4)
N(1)-Ir(1)-O(1)	91.8 (2)	N(2)-Ir(1)-O(1)	93.3 (2)	Se(1)-C(12)	1.918 (8)
O(2)-Ir(1)-O(1)	88.6 (2)	C(12)-Se(1)-C(9)	99.2 (4)	Se(1)-C(9)	1.926 (11)
C(26)-Se(2)-C(23)	86.2 (4)			Se(2)-C(26)	1.852 (11)
				Se(2)-C(23)	1.882 (7)

Table S3. Selected structural parameters of **IrSe-3F**.

Bond angles (°)				Bond lengths (Å)	
C(20)-Ir(1)-C(7)	91.8 (2)	C(20)-Ir(1)-N(1)	93.4 (2)	Ir(1)-C(20)	1.986 (5)
C(7)-Ir(1)-N(1)	80.91 (19)	C(20)-Ir(1)-N(2)	80.6 (2)	Ir(1)-C(7)	1.991 (5)
C(7)-Ir(1)-N(2)	96.29 (19)	N(1)-Ir(1)-N(2)	173.3 (17)	Ir(1)-N(1)	2.037 (4)
C(20)-Ir(1)-O(2)	174.06 (18)	C(7)-Ir(1)-O(2)	90.45 (18)	Ir(1)-N(2)	2.062 (4)
N(1)-Ir(1)-O(2)	92.42 (16)	N(2)-Ir(1)-O(2)	93.69 (17)	Ir(1)-O(2)	2.139 (4)
C(20)-Ir(1)-O(1)	90.63 (18)	C(7)-Ir(1)-O(1)	174.08 (18)	Ir(1)-O(1)	2.141 (4)
N(1)-Ir(1)-O(1)	93.54 (17)	N(2)-Ir(1)-O(1)	89.44 (16)	Se(1)-C(18)	1.856 (7)
O(2)-Ir(1)-O(1)	87.70 (15)	C(18)-Se(1)-C(21)	85.6 (3)	Se(1)-C(21)	1.882(5)
C(12)-Se(2)-C(9)	101.6 (2)			Se(2)-C(12)	1.918 (6)
				Se(2)-C(9)	1.921 (6)

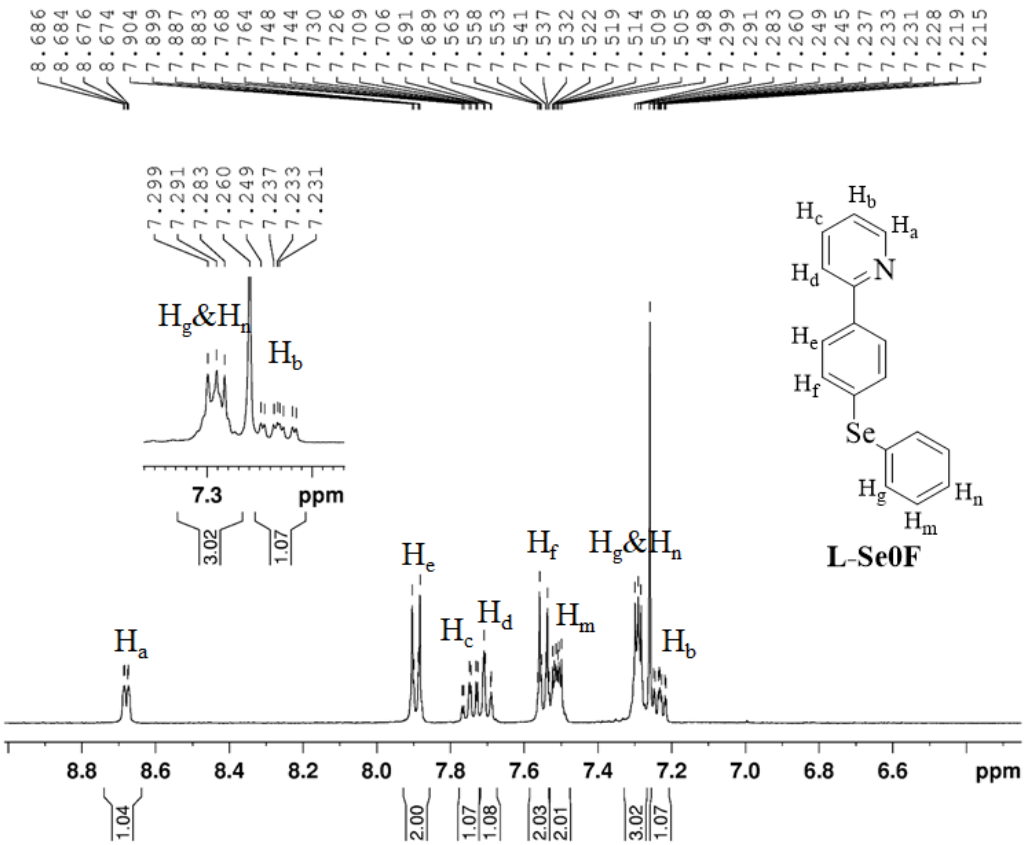
8.686
8.684
8.676
8.674
7.904
7.899
7.887
7.883
7.768
7.764
7.748
7.744
7.730
7.726
7.709
7.706
7.691
7.689
7.563
7.558
7.553
7.541
7.537
7.532
7.522
7.519
7.514
7.509
7.505
7.498
7.299
7.291
7.283
7.260
7.249
7.245
7.237
7.233
7.231
7.228
7.219
7.215
Hg&Hn
Hb
7.3
ppm
3.02
1.07
Hc
Hb
Ha
Hd
N
He
Hf
Se
Hg
Hn
Hm
L-Se0F
Ha
Hc
Hd
He
Hm
Hf
Hg&Hn
Hb
8.8
8.6
8.4
8.2
8.0
7.8
7.6
7.4
7.2
7.0
6.8
6.6
ppm
1.04
2.00
1.07
1.08
2.03
2.01
3.02
1.07

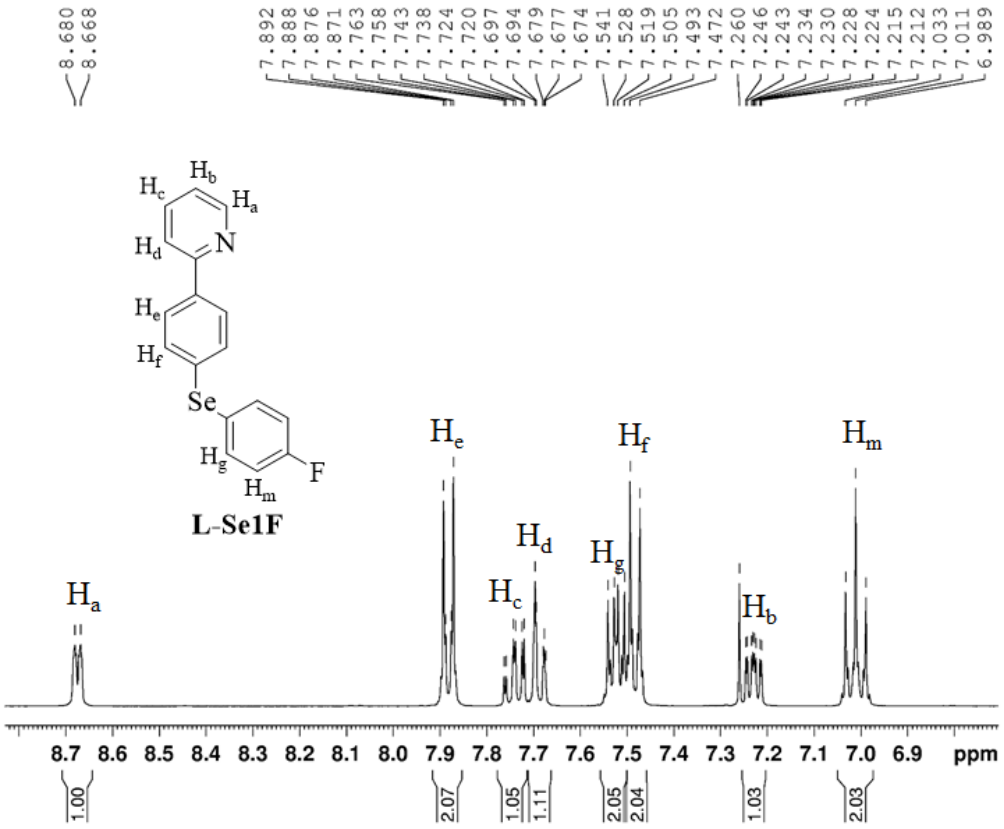
8.680
8.668
7.892
7.888
7.876
7.871
7.763
7.758
7.743
7.738
7.724
7.720
7.697
7.694
7.679
7.677
7.674
7.541
7.528
7.519
7.505
7.493
7.472
7.260
7.246
7.243
7.234
7.230
7.228
7.224
7.215
7.212
7.033
7.011
6.989
Hc
Hb
Ha
Hd
N
He
Hf
Se
Hg
F
Hm
L-Se1F
Ha
He
Hc
Hd
Hg
Hf
Hb
Hm
8.7
8.6
8.5
8.4
8.3
8.2
8.1
8.0
7.9
7.8
7.7
7.6
7.5
7.4
7.3
7.2
7.1
7.0
6.9
ppm
1.00
2.07
1.05
1.11
2.05
2.04
1.03
2.03

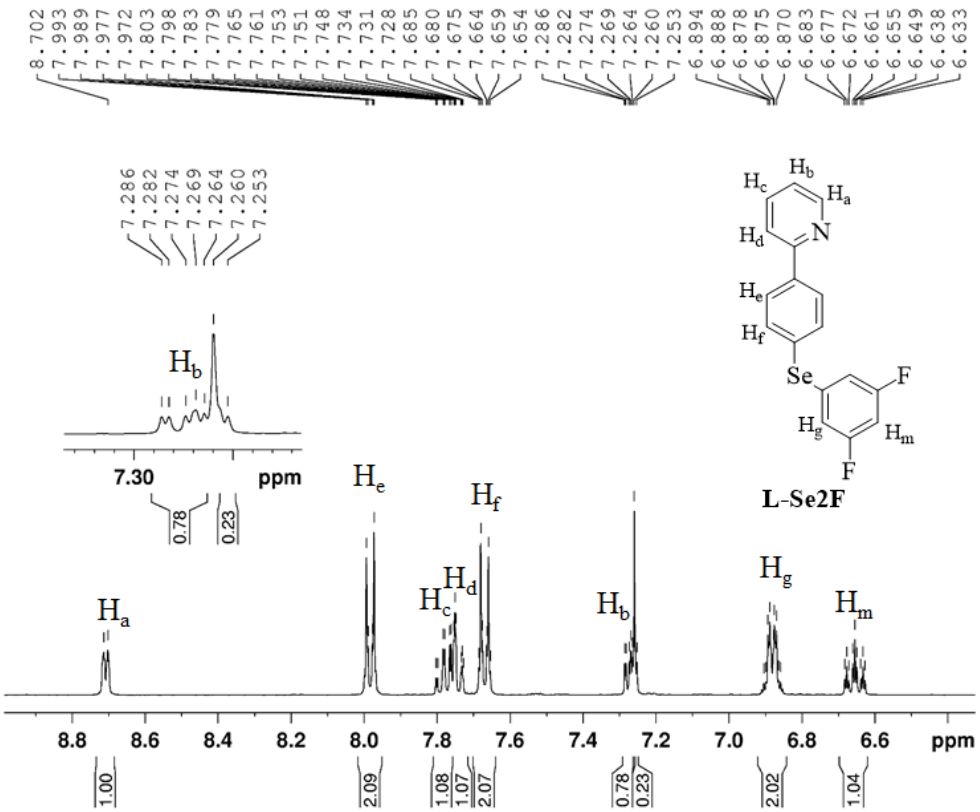
8.702
7.993
7.989
7.977
7.972
7.803
7.798
7.783
7.779
7.765
7.761
7.753
7.751
7.748
7.734
7.731
7.728
7.685
7.680
7.675
7.664
7.659
7.654
7.286
7.282
7.274
7.269
7.264
7.260
7.253
6.894
6.888
6.878
6.875
6.870
6.683
6.677
6.672
6.661
6.655
6.649
6.638
6.633
Hb
7.30
ppm
0.78
0.23
He
Hf
Hc
Hd
Ha
Hb
Hg
Hm
8.8
8.6
8.4
8.2
8.0
7.8
7.6
7.4
7.2
7.0
6.8
6.6
ppm
1.00
2.09
1.08
1.07
2.07
0.78
0.23
2.02
1.04
L-Se2F

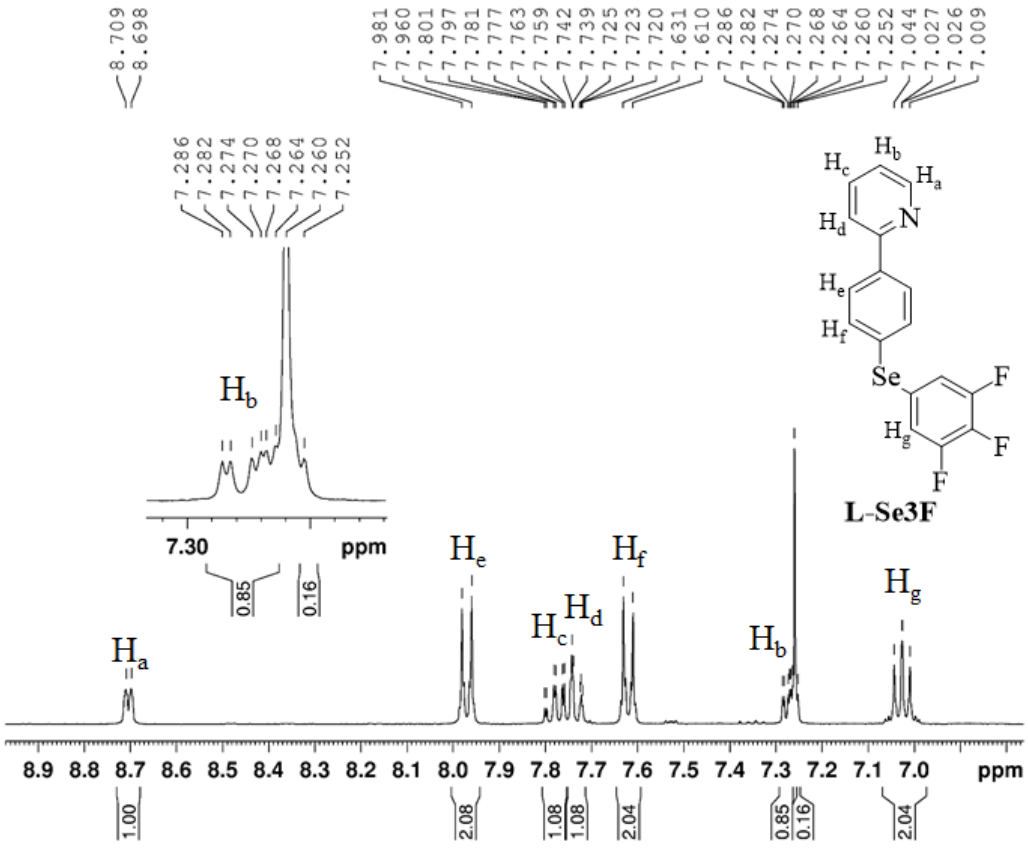
8.709
8.698
7.981
7.960
7.801
7.797
7.781
7.777
7.763
7.759
7.742
7.739
7.725
7.723
7.720
7.631
7.610
7.286
7.282
7.274
7.270
7.268
7.264
7.260
7.252
7.044
7.027
7.026
7.009
Hb
7.30
ppm
0.85
0.16
He
Hf
Hc
Hd
Ha
Hb
Hg
8.9
8.8
8.7
8.6
8.5
8.4
8.3
8.2
8.1
8.0
7.9
7.8
7.7
7.6
7.5
7.4
7.3
7.2
7.1
7.0
ppm
1.00
2.08
1.08
1.08
2.04
0.85
0.16
2.04
L-Se3F

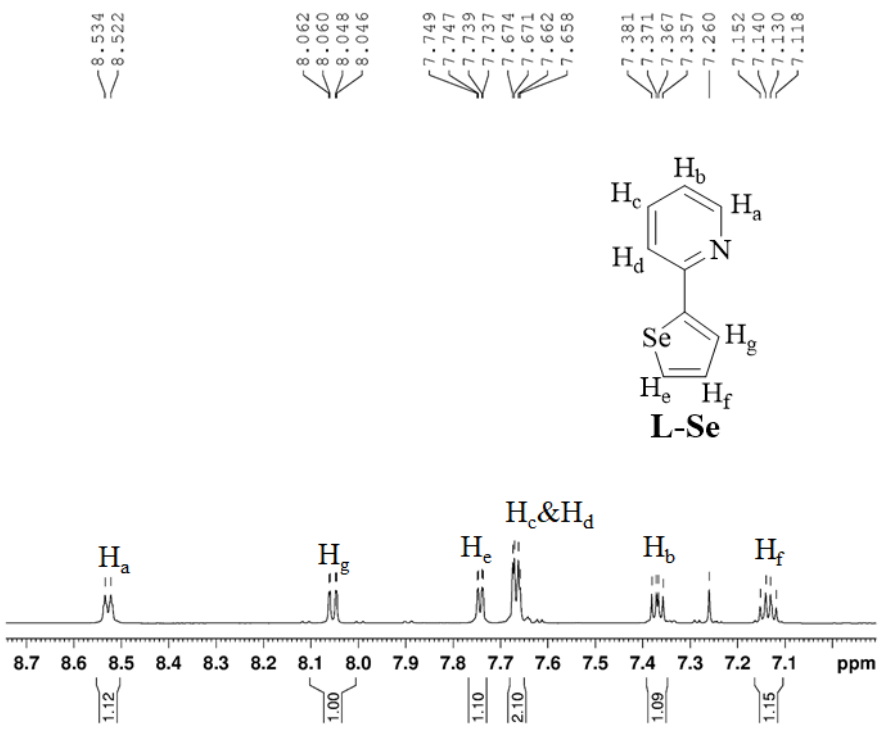

Figure S1. [1]H-NMR spectra for **L-Se0F** – **L-Se3F** and **L-Se**. Full assignment of the resonance signals observed is presented.

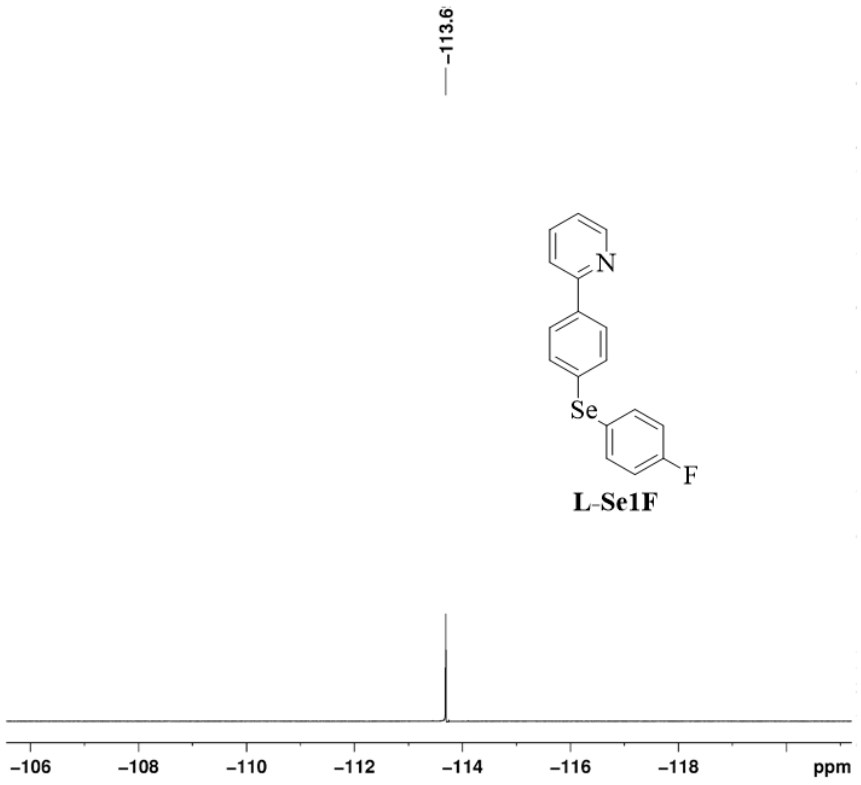

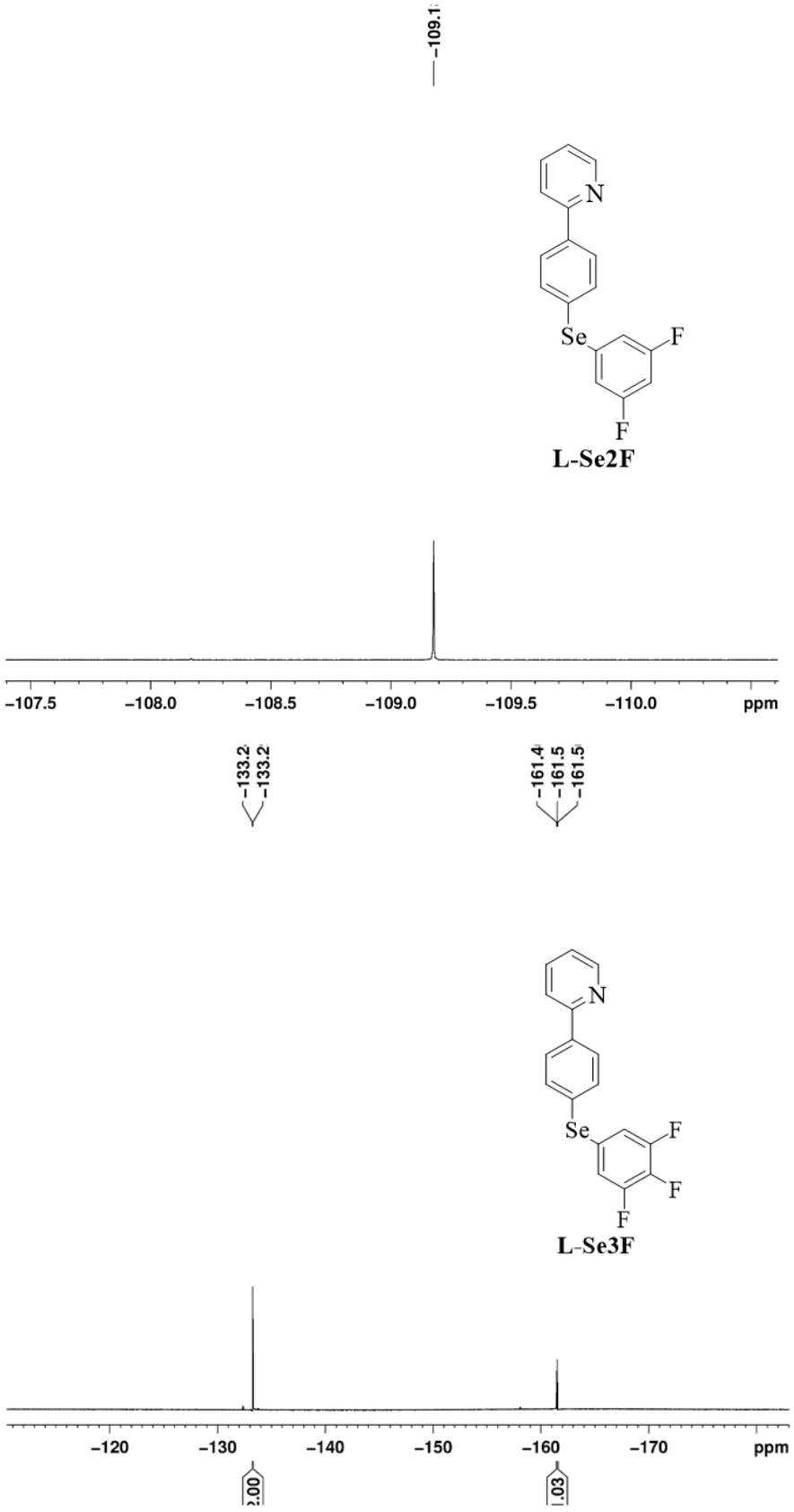

Figure S2. ^{19}F-NMR spectra for **L-Se1F** – **L-Se3F**.

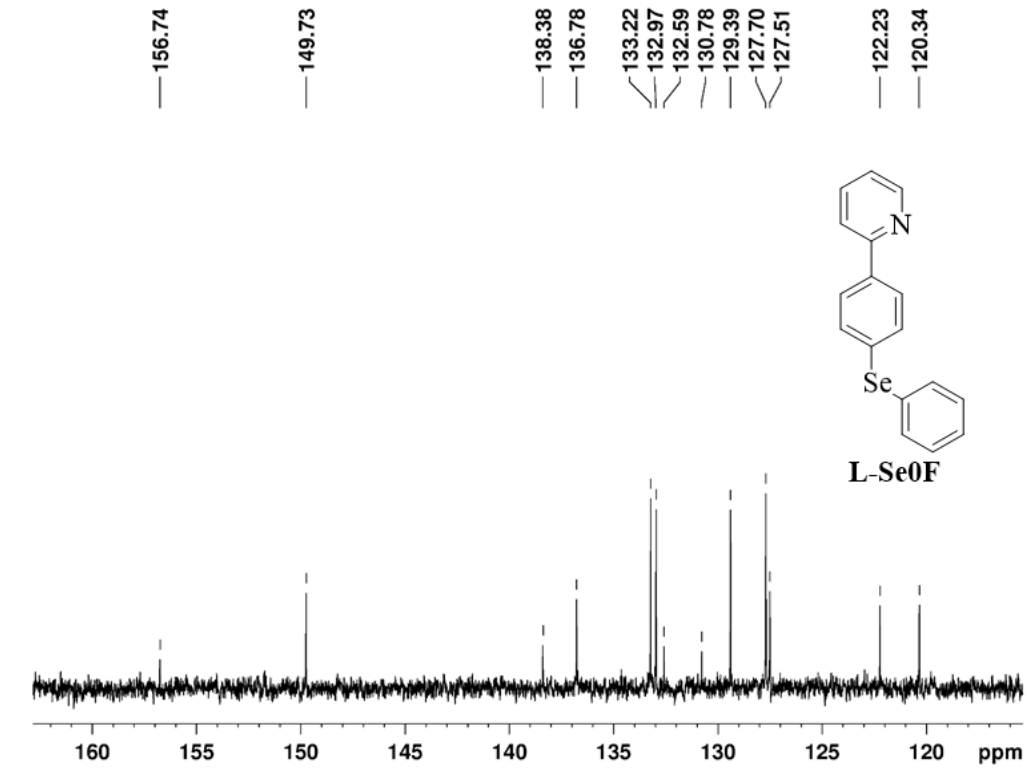
156.74
149.73
138.38
136.78
133.22
132.97
132.59
130.78
129.39
127.70
127.51
122.23
120.34
N
Se
L-Se0F
160
155
150
145
140
135
130
125
120
ppm

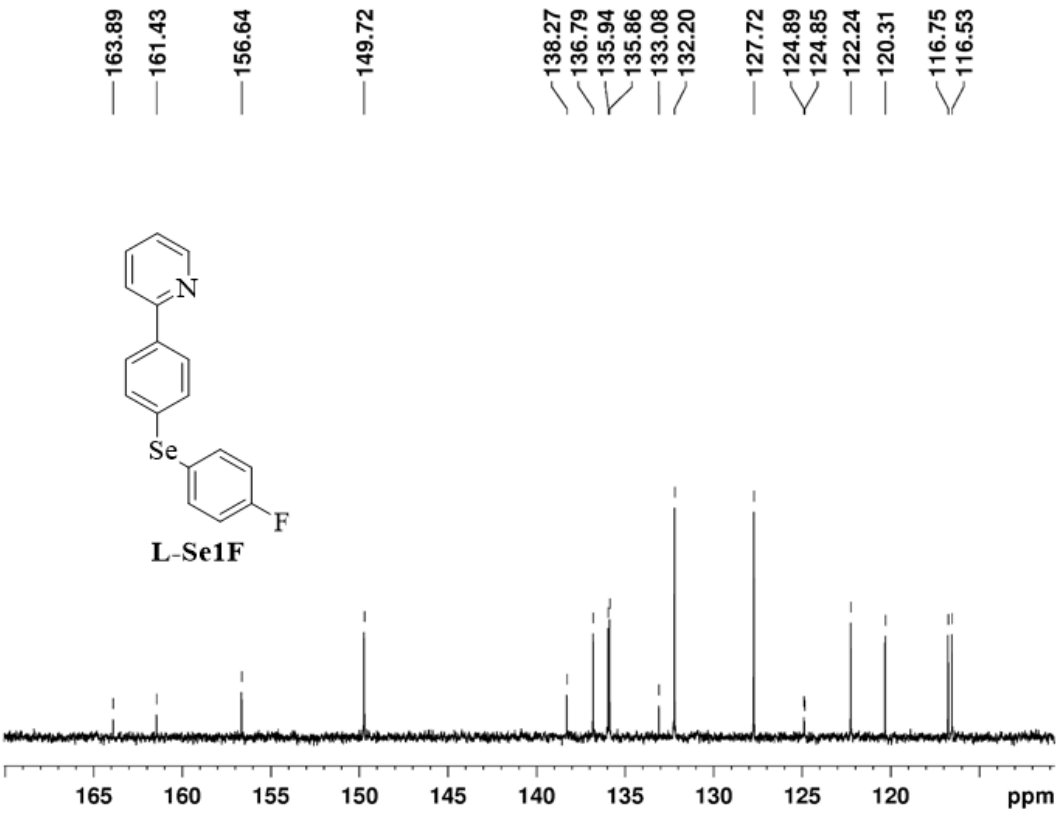
163.89
161.43
156.64
149.72
138.27
136.79
135.94
135.86
133.08
132.20
127.72
124.89
124.85
122.24
120.31
116.75
116.53
N
Se
F
L-Se1F
165
160
155
150
145
140
135
130
125
120
ppm

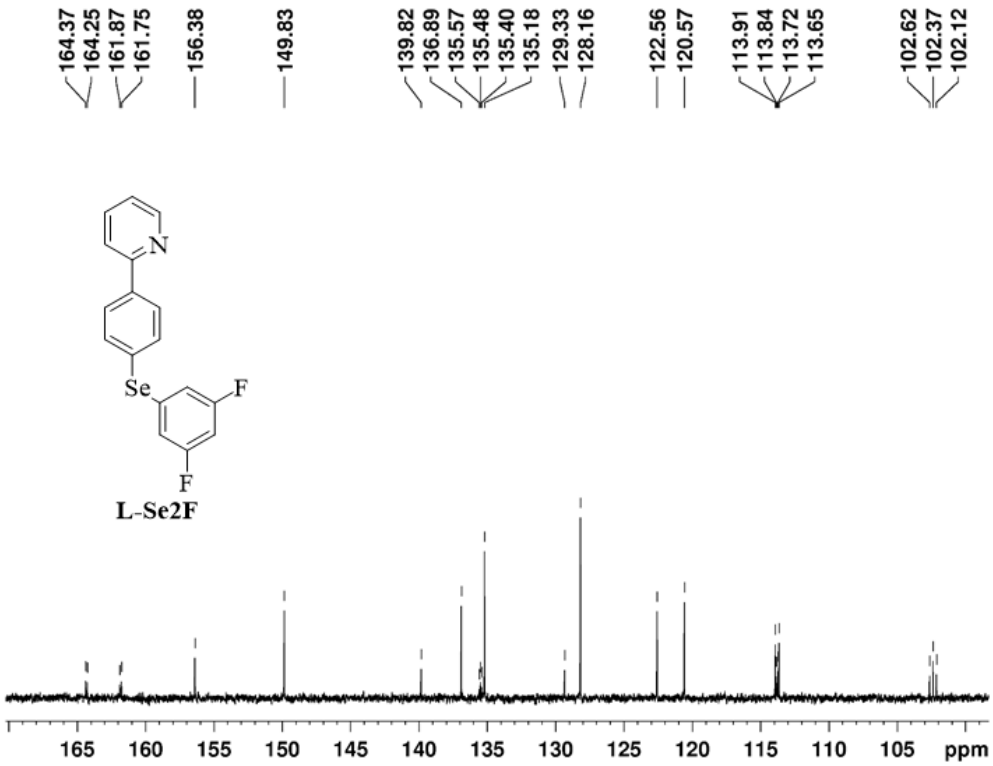
164.37
164.25
161.87
161.75
156.38
149.83
139.82
136.89
135.57
135.48
135.40
135.18
129.33
128.16
122.56
120.57
113.91
113.84
113.72
113.65
102.62
102.37
102.12
N
Se
F
F
L-Se2F
165
160
155
150
145
140
135
130
125
120
115
110
105
ppm

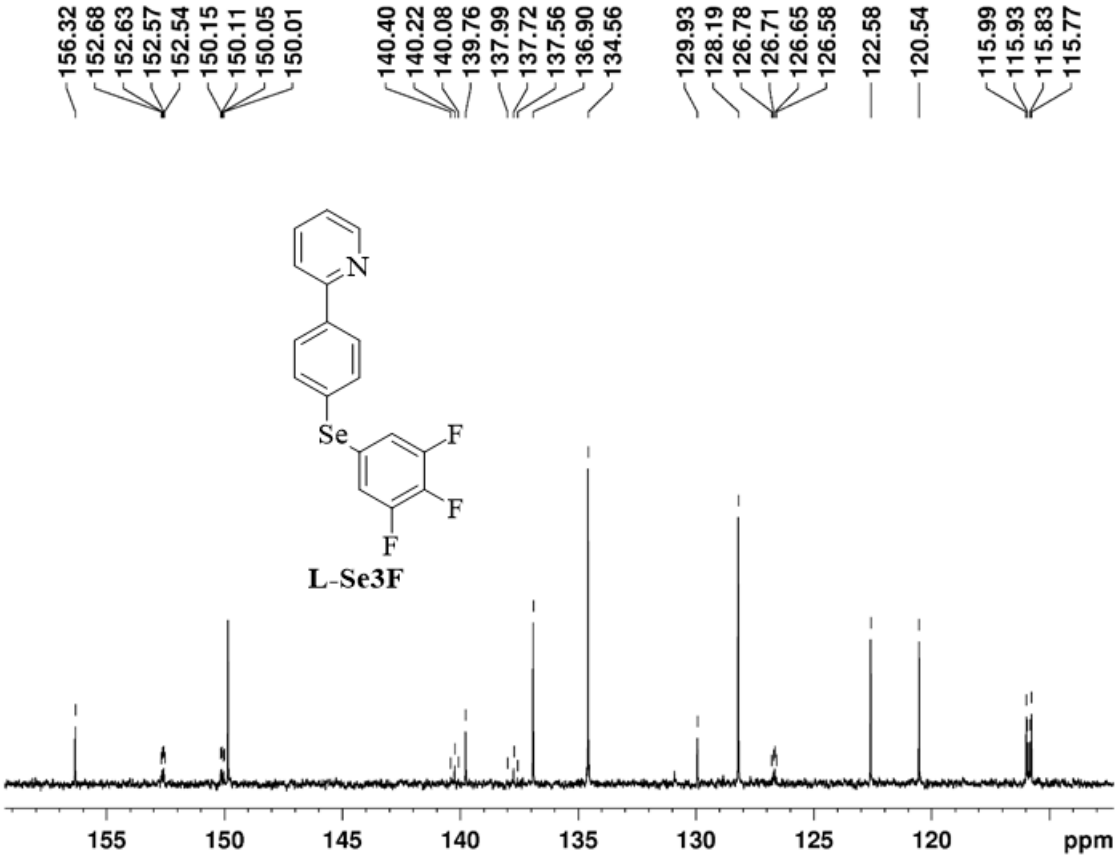
156.32
152.68
152.63
152.57
152.54
150.15
150.11
150.05
150.01
140.40
140.22
140.08
139.76
137.99
137.72
137.56
136.90
134.56
129.93
128.19
126.78
126.71
126.65
126.58
122.58
120.54
115.99
115.93
115.83
115.77
N
Se
F
F
F
L-Se3F
155
150
145
140
135
130
125
120
ppm

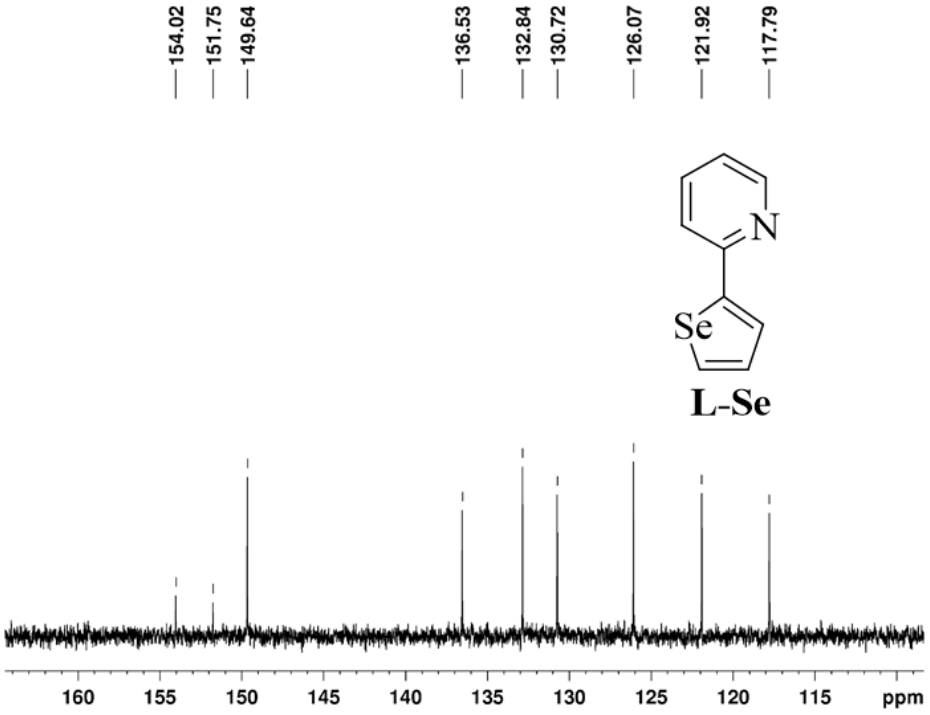

Figure S3. ^{13}C-NMR spectra for **L-Se0F** – **L-Se3F** and **L-Se**.

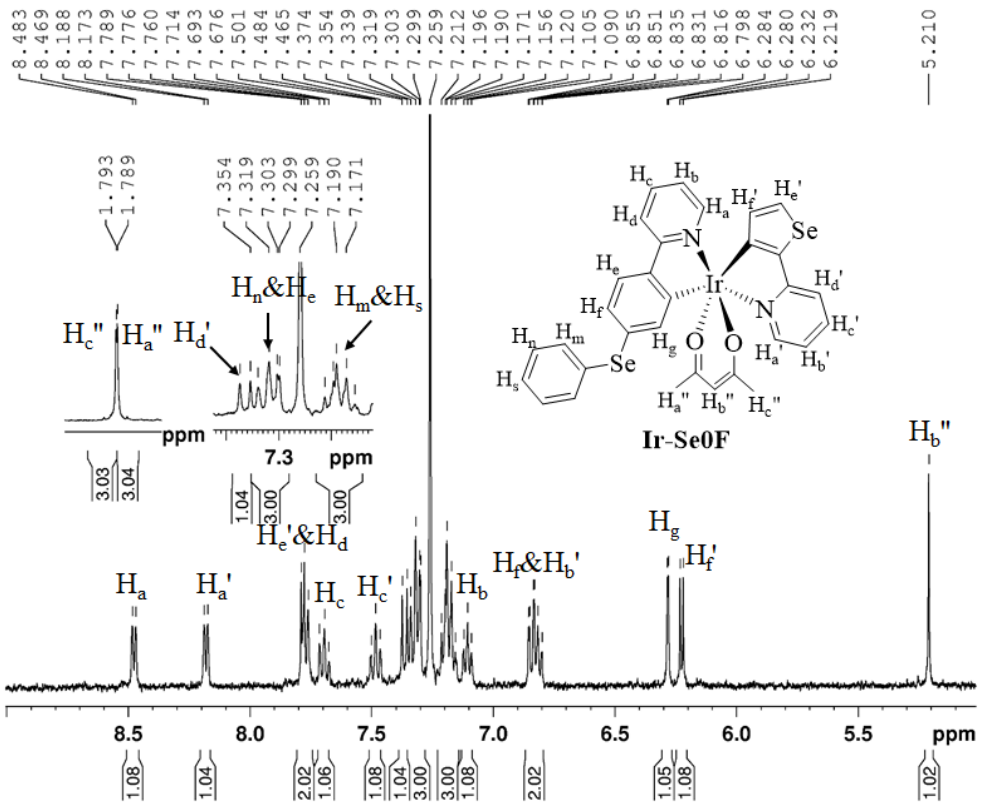

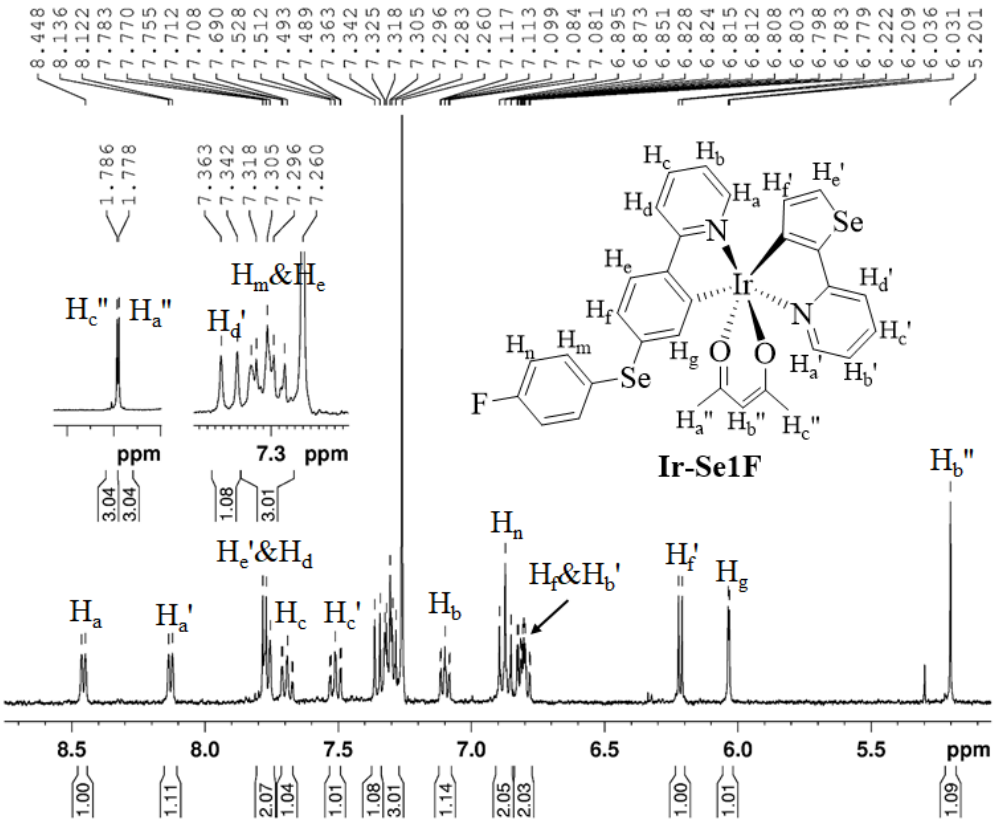
Ir-Se1F
ppm
7.3 ppm
8.5
8.0
7.5
7.0
6.5
6.0
5.5
ppm

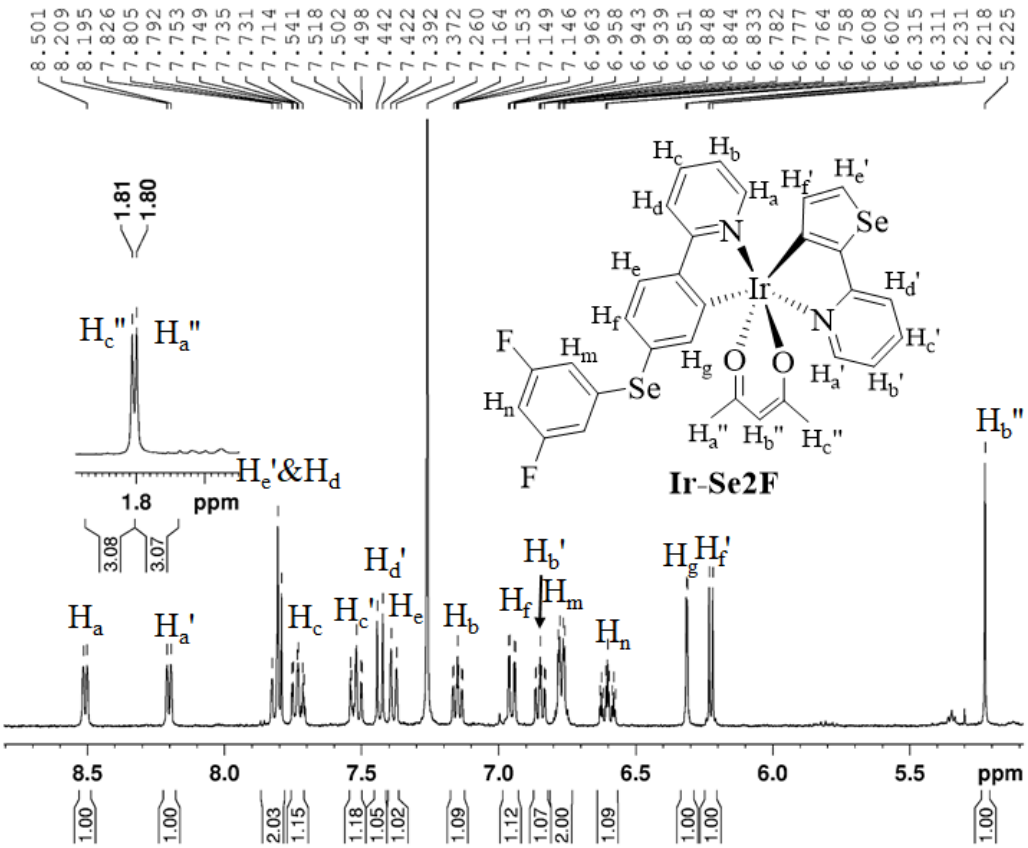
Ir-Se2F
1.8 ppm
8.5
8.0
7.5
7.0
6.5
6.0
5.5
ppm

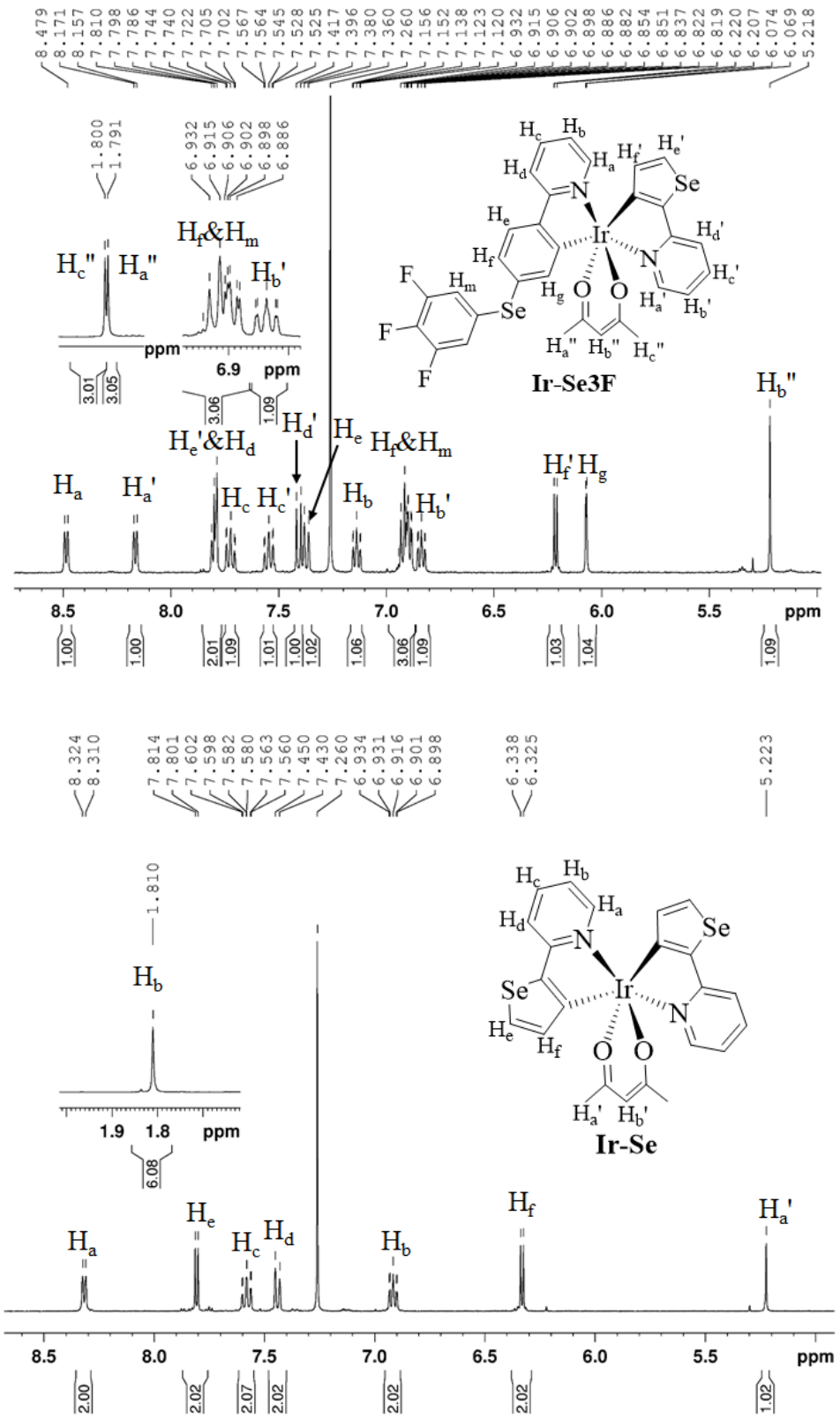

Figure S4. [1]H-NMR spectra for **Ir-Se0F** – **Ir-Se3F** and **Ir-Se**. Full assignment of the resonance signals observed is presented.

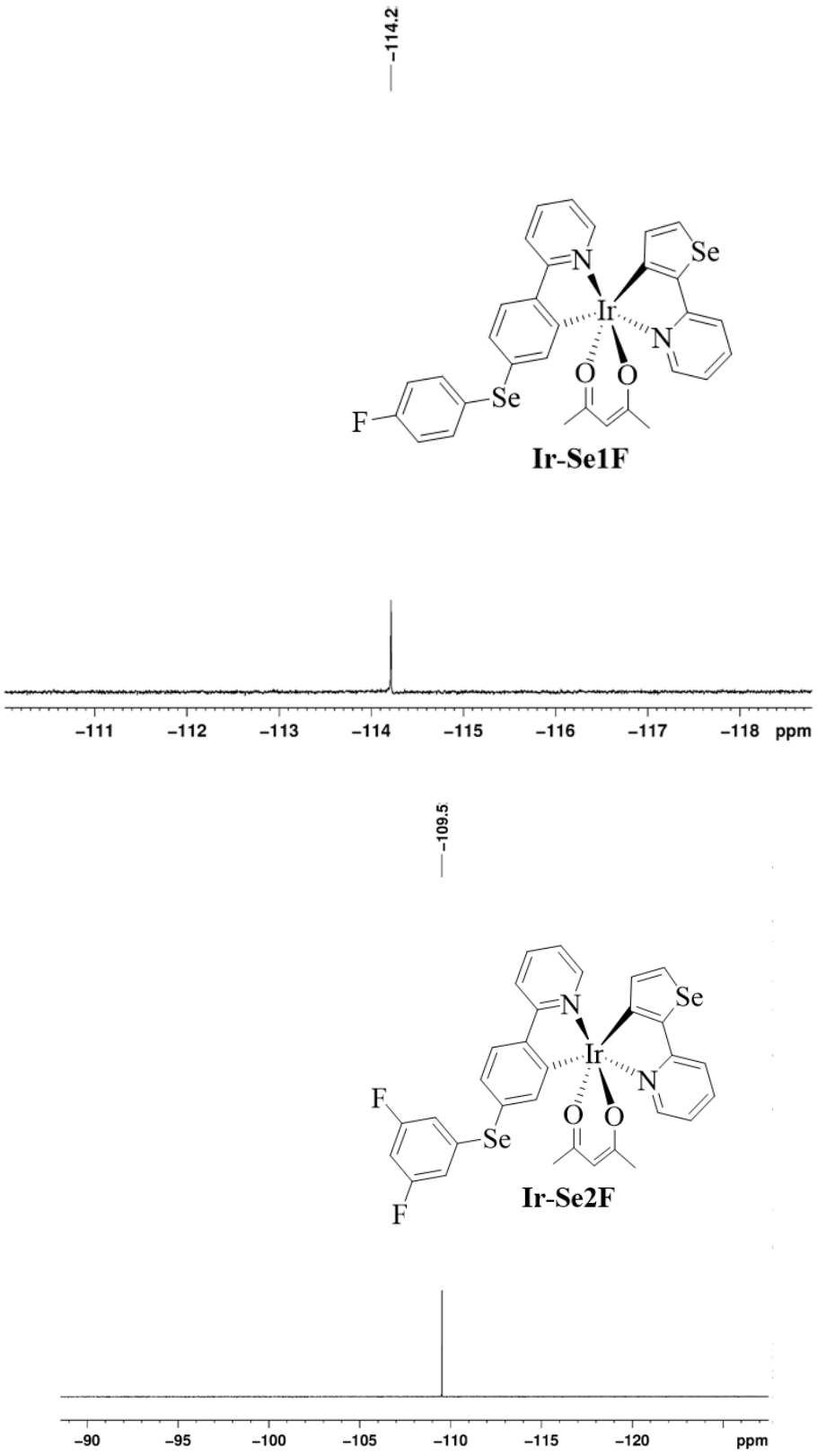
−114.2
N
Ir
Se
N
O
O
Se
F
Ir-Se1F
−111
−112
−113
−114
−115
−116
−117
−118
ppm
−109.5
N
Ir
Se
N
O
O
F
Se
F
Ir-Se2F
−90
−95
−100
−105
−110
−115
−120
ppm

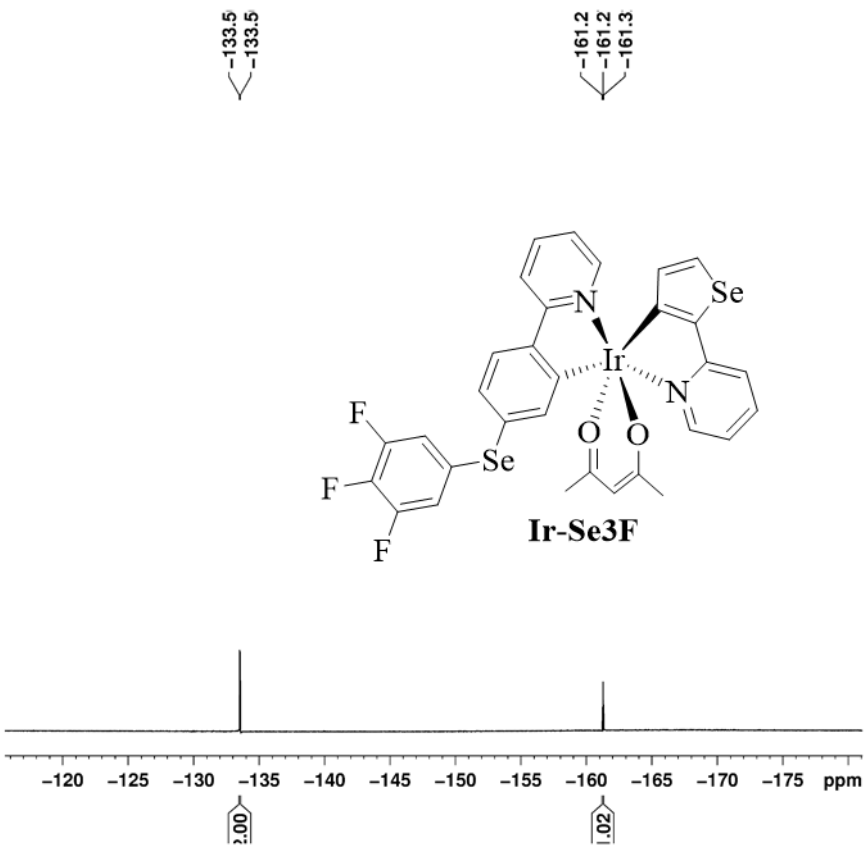

Figure S5. ^{19}F-NMR spectra for **Ir-Se1F** – **Ir-Se3F**.

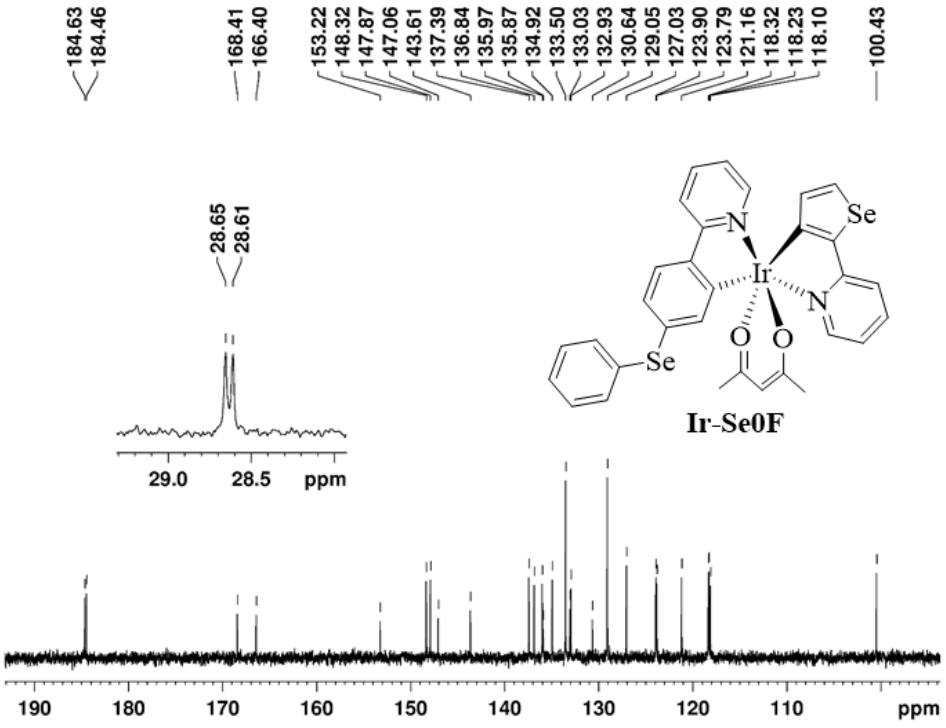

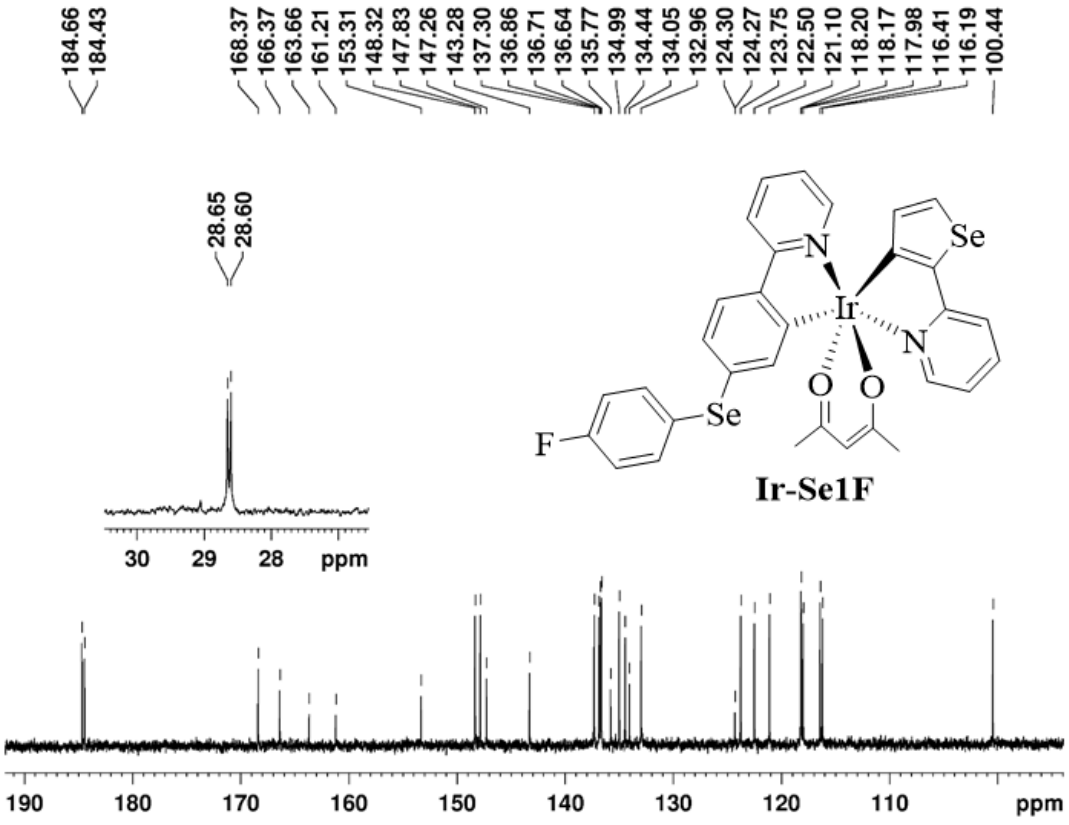
184.66
184.43
168.37
166.37
163.66
161.21
153.31
148.32
147.83
147.26
143.28
137.30
136.86
136.71
136.64
135.77
134.99
134.44
134.05
132.96
124.30
124.27
123.75
122.50
121.10
118.20
118.17
117.98
116.41
116.19
100.44
28.65
28.60
30
29
28
ppm
N
Ir
Se
N
O
O
Se
F
Ir-Se1F
190
180
170
160
150
140
130
120
110
ppm

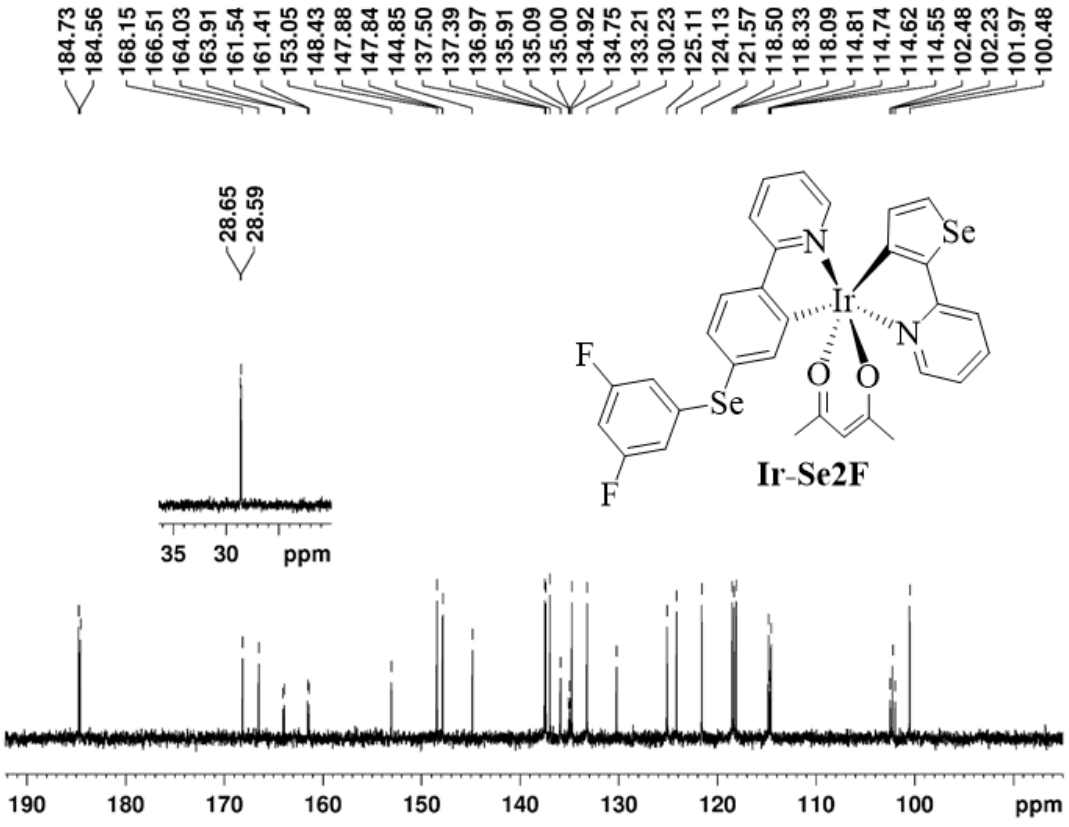
184.73
184.56
168.15
166.51
164.03
163.91
161.54
161.41
153.05
148.43
147.88
147.84
144.85
137.50
137.39
136.97
135.91
135.09
135.00
134.92
134.75
133.21
130.23
125.11
124.13
121.57
118.50
118.33
118.09
114.81
114.74
114.62
114.55
102.48
102.23
101.97
100.48
28.65
28.59
35
30
ppm
N
Ir
Se
N
O
O
F
Se
F
Ir-Se2F
190
180
170
160
150
140
130
120
110
100
ppm

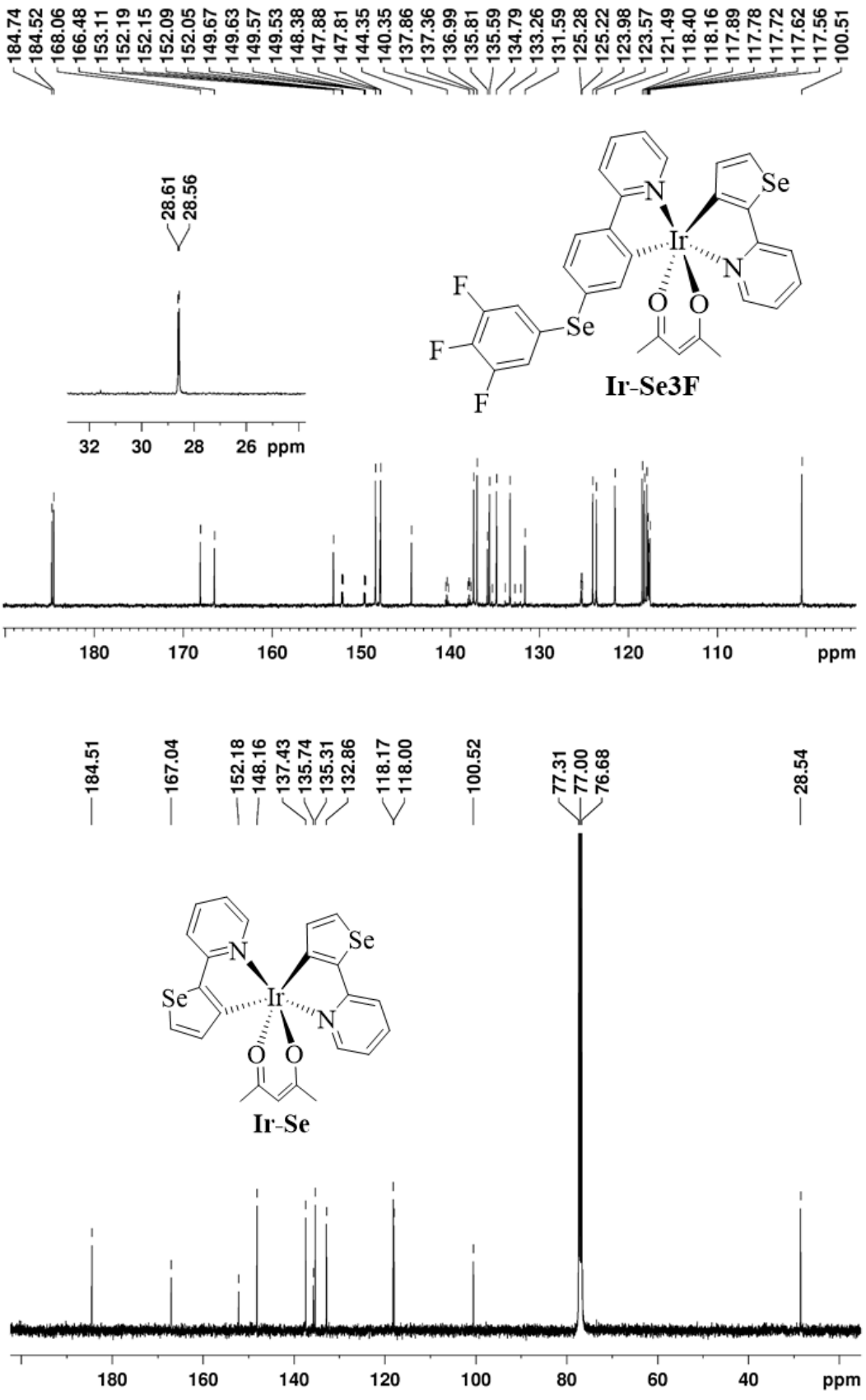

Figure S6. ^{13}C-NMR spectra for **Ir-Se1F** – **Ir-Se3F** and **Ir-Se**.

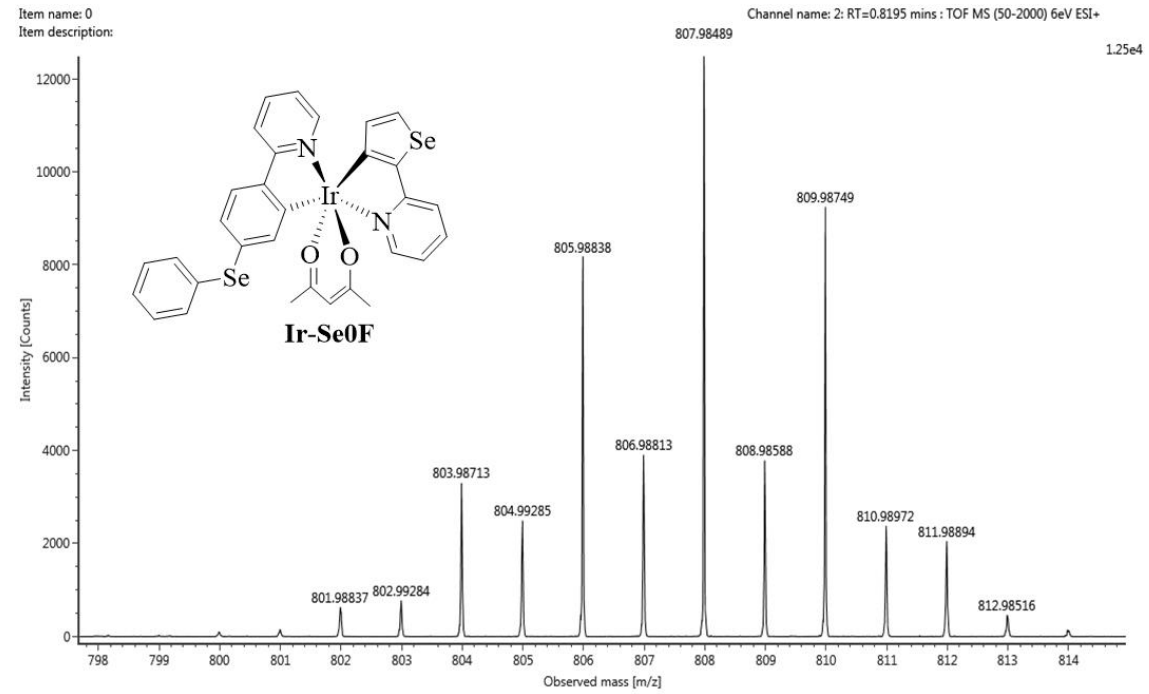

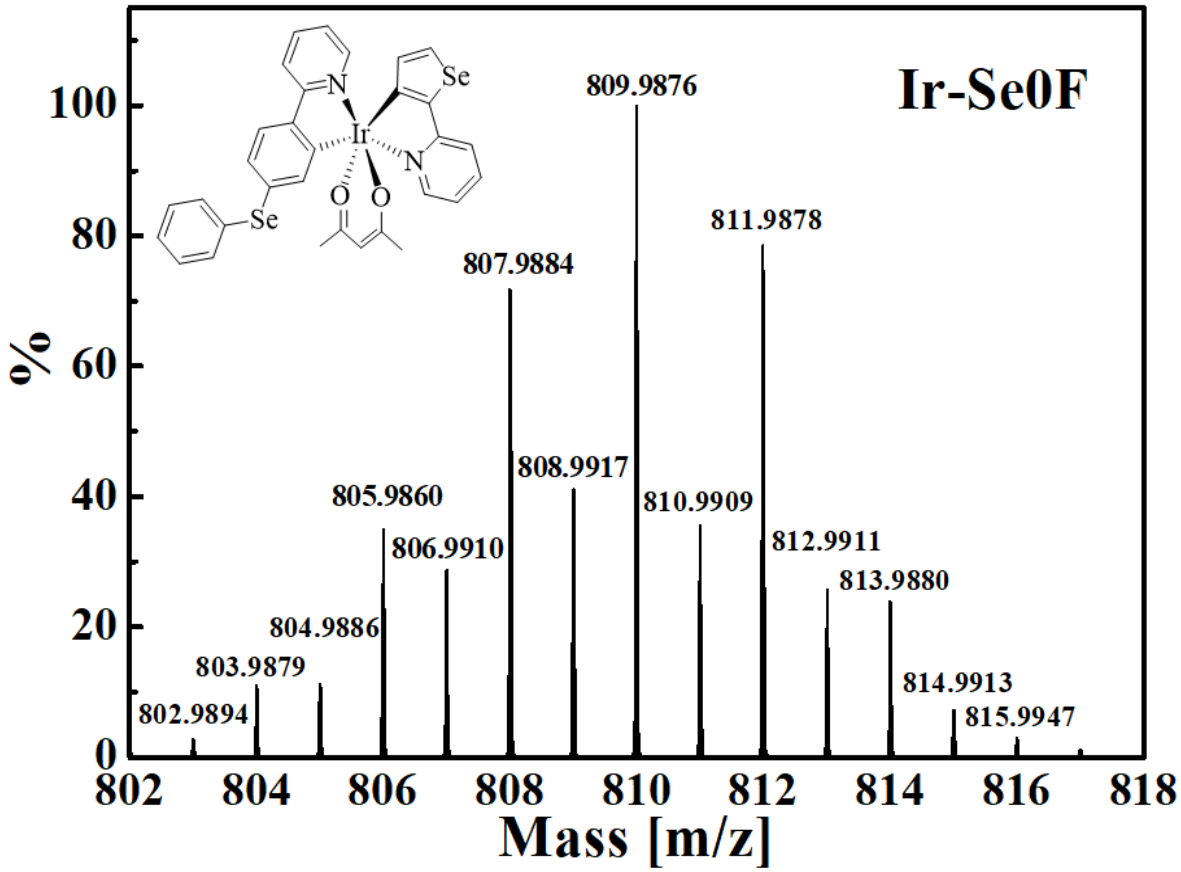

(a) Up: experimental; Down: Calculated.

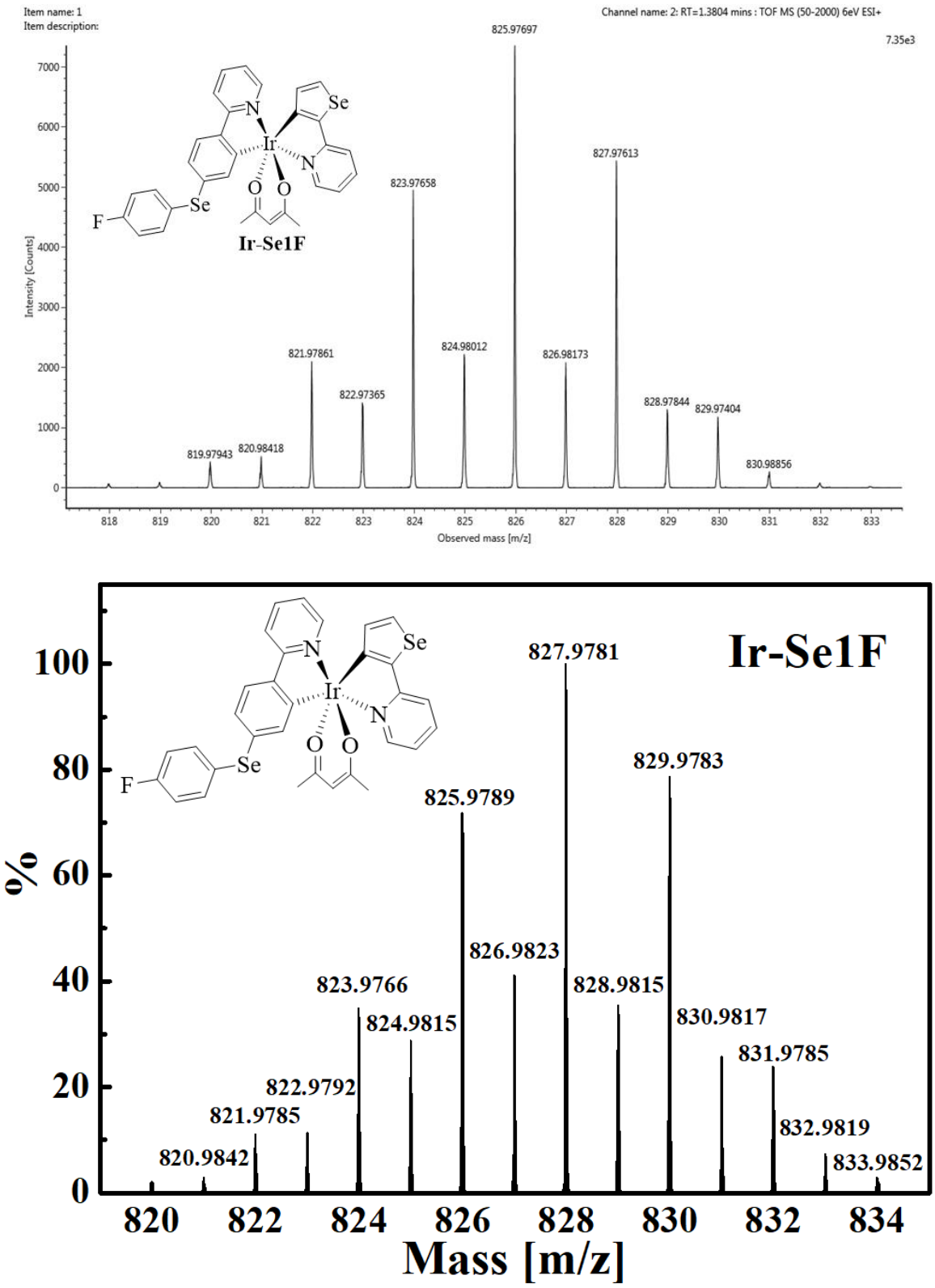

(b) Up: experimental; Down: Calculated.

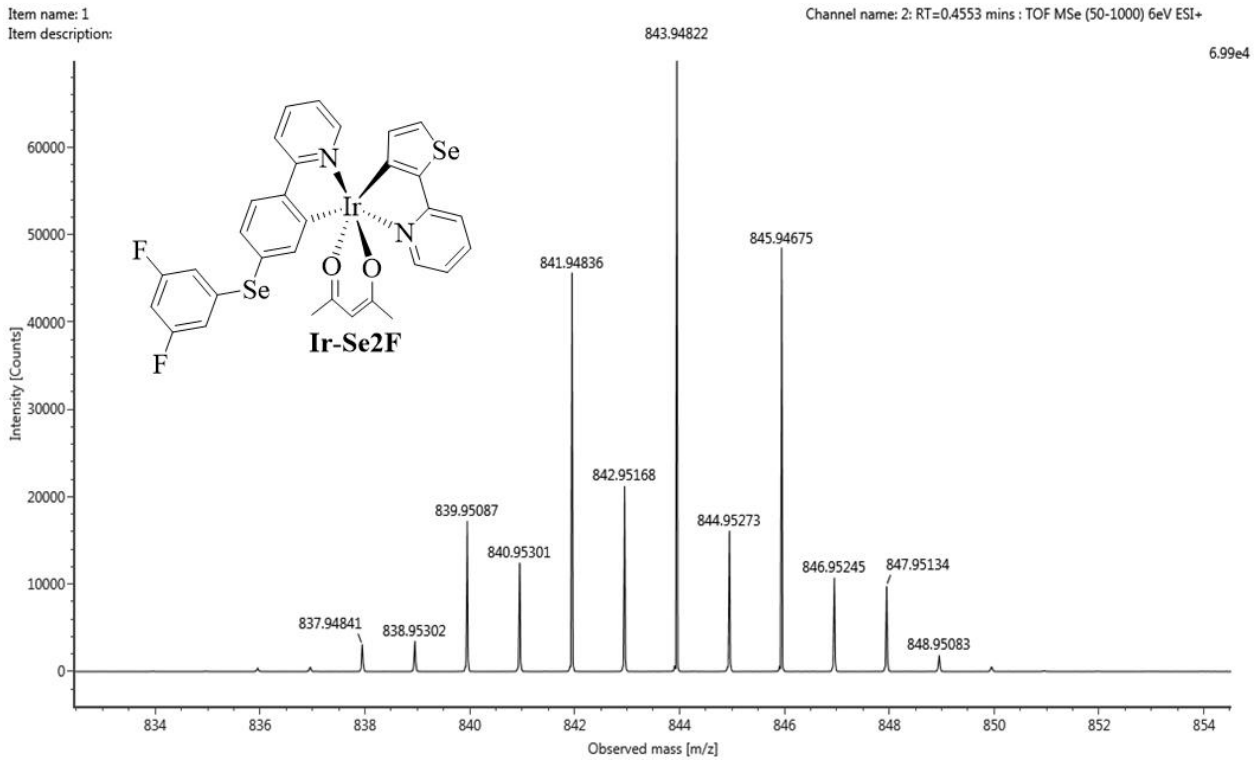

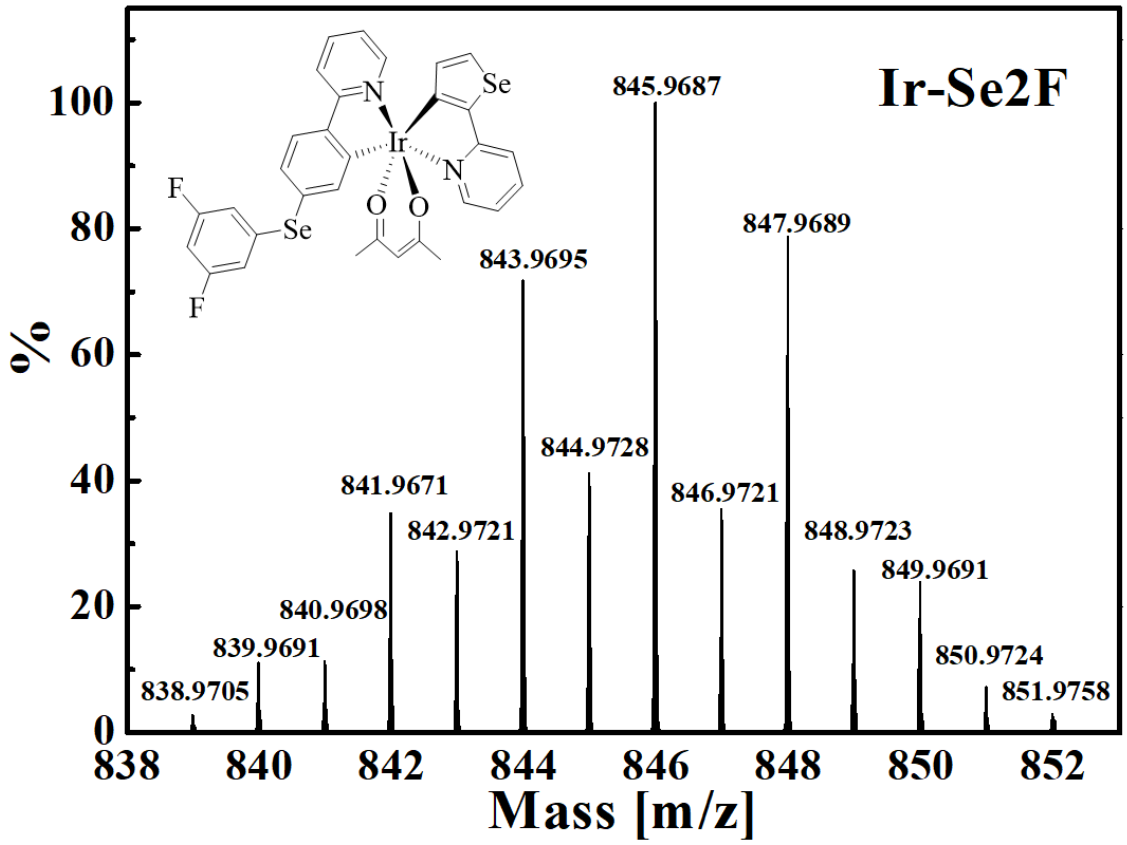

(c) Up: experimental; Down: Calculated.

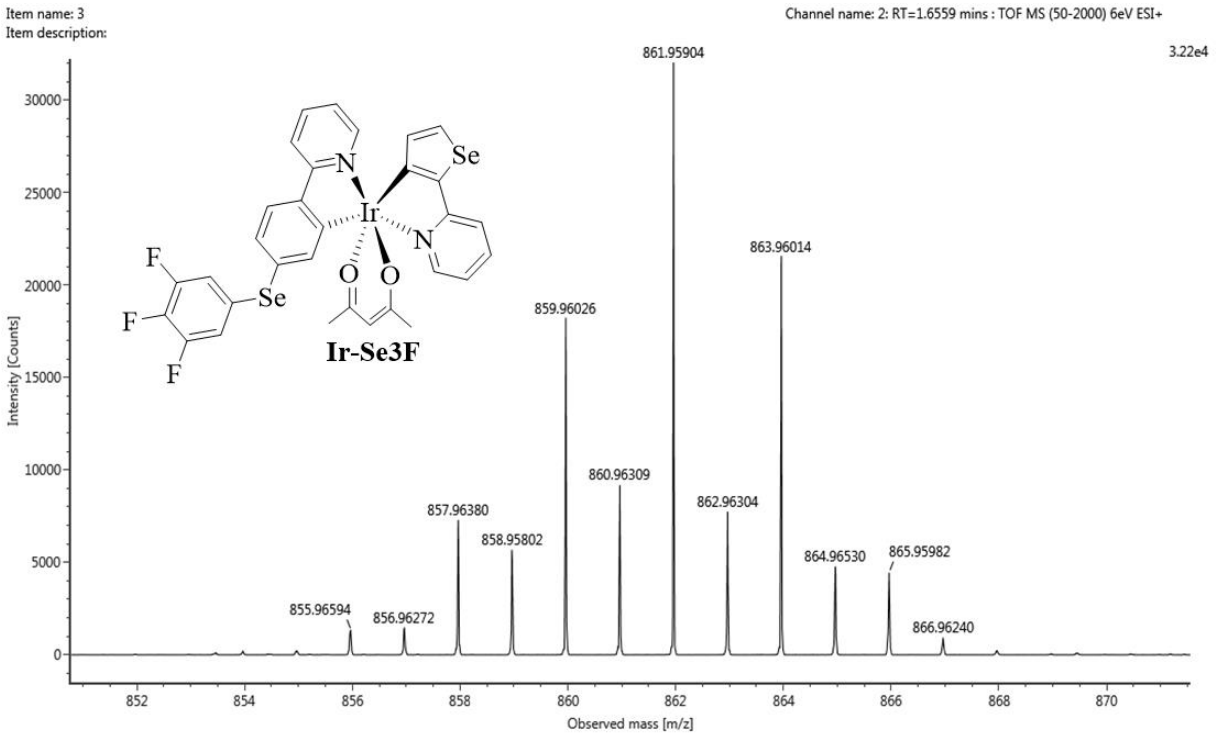

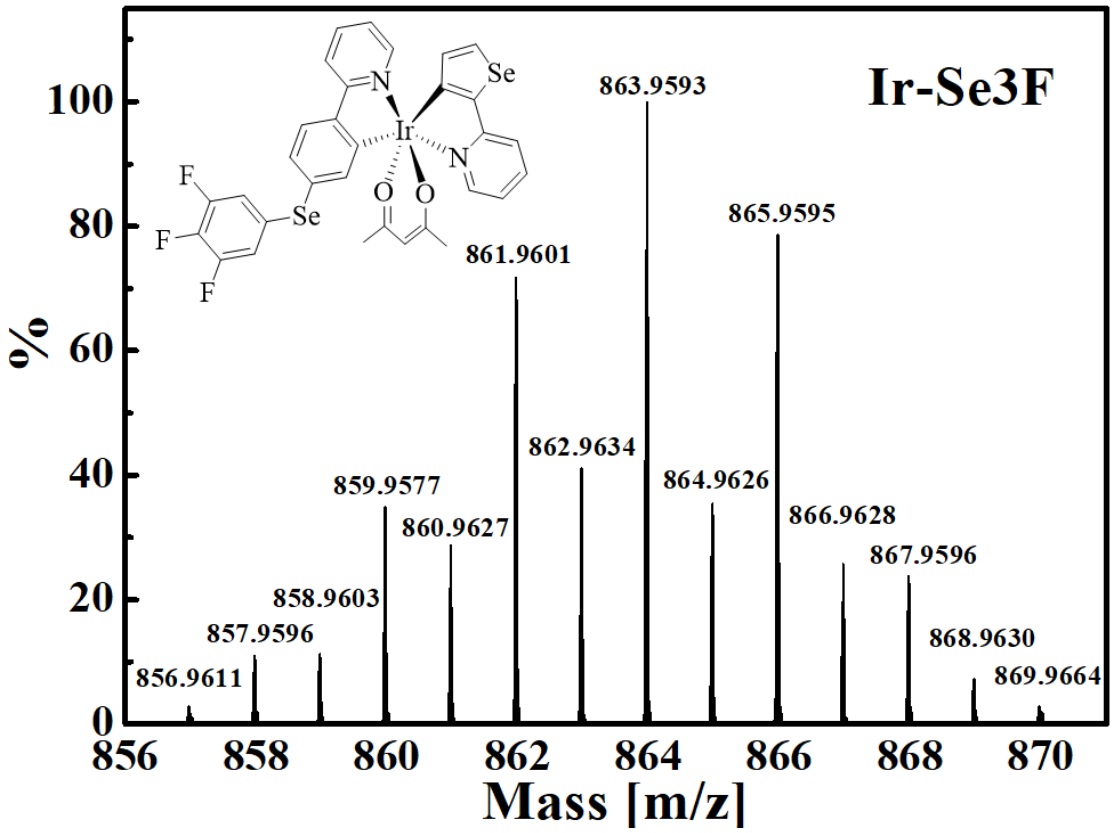

(d) Up: experimental; Down: Calculated.

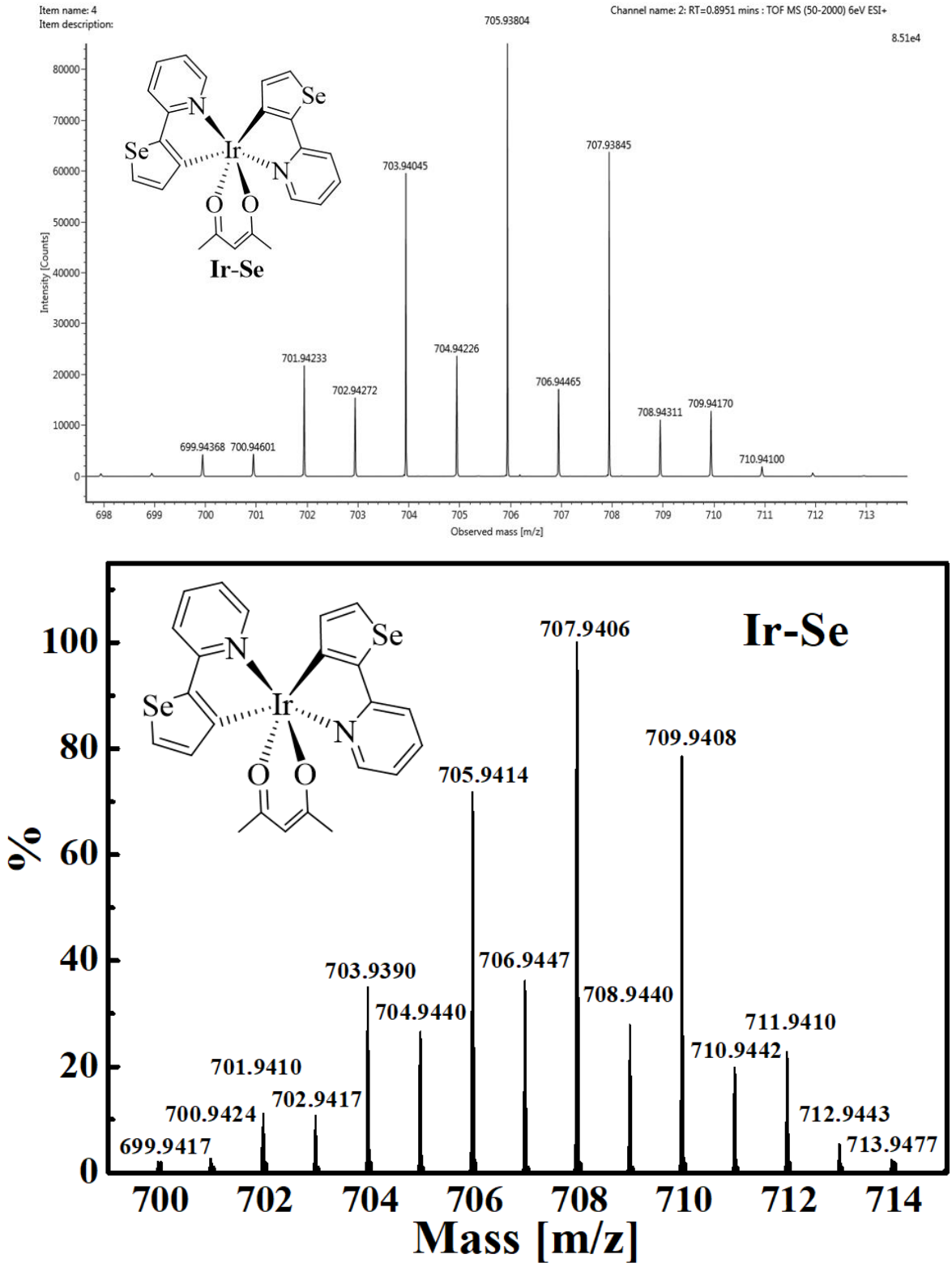

(e) Up: experimental; Down: Calculated.

Figure S7. Experimental HRMS and Calculated spectral pattern (isotopic distribution) of **Ir-Se0F** – **Ir-Se3F** and **Ir-Se**. (a) **Ir-Se0F**; (b) **Ir-Se1F**; (c) **Ir-Se2F**; (d) **Ir-Se3F**; (e) **Ir-Se**.

Table S4. Photophysical of the Asymmetric Heteroleptic Ir(III) Complexes and Their Parent Complex **Ir-Se**.

	Excitation λ_{max} (nm) [a]	Emission (film) λ_{em} (nm)		Φ_P [d]	τ (μs) [e]	T_d/T_g (°C)
		Film [b]	77 K [c]			
Ir-Se0F	336 (584 nm)	584, 630, 696^{sh}	578，629，691^{sh}	90.7	3.18 (584 nm)	278/110
Ir-Se1F	337 (584 nm)	584, 633, 696^{sh}	575, 626, 688^{sh}	91.4	3.04 (584 nm)	276/112
Ir-Se2F	336 (584 nm)	584, 629, 697^{sh}	576, 627, 689^{sh}	90.5	3.09 (584 nm)	283/113
Ir-Se3F	337 (584 nm)	584, 631, 695^{sh}	575, 626, 687^{sh}	92.3	3.35 (584 nm)	292/115
Ir-Se	337 (592 nm)	592, 636, 702^{sh}	583, 634, 699^{sh}	61.1	3.38 (592 nm)	292/115

[a] Measured in an 8 wt% doped CBP film. λ_{max} represents the excitation wavelength at which the maximum emission intensity of the monitoring wavelength is obtained. The monitoring wavelength in parentheses is presented. [b] Measured in an 8 wt% doped CBP film, λ_{ex} = 380 nm. sh: shoulder. [c] Measured in CH_2Cl_2 solution at a 10^{-5} M. sh: shoulder. [d] Measured with an integrating sphere in an 8 wt% doped CBP film. [e] Measured in an 8 wt% doped CBP film and the monitoring wavelength in parentheses is presented.

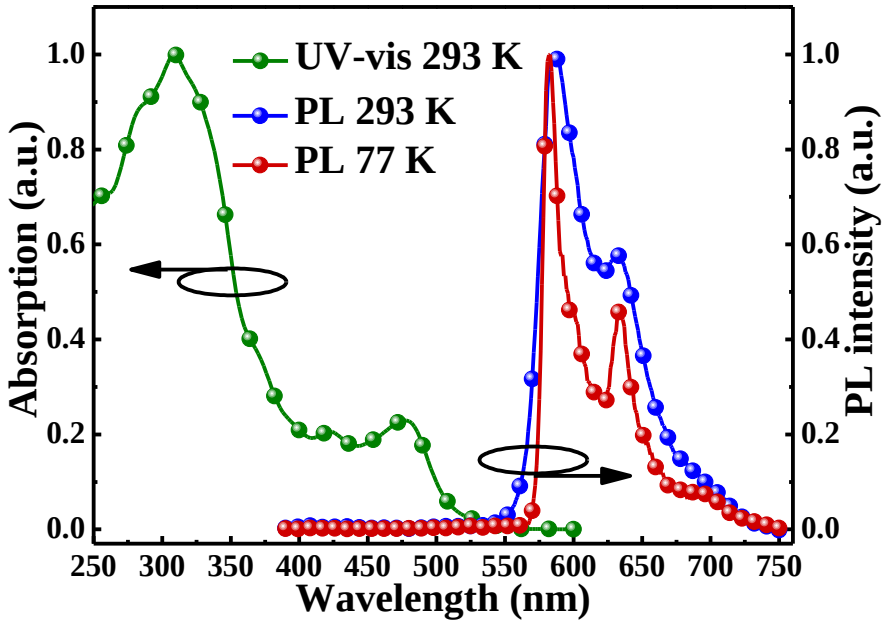

Figure S8. UV-vis absorption spectra and photoluminescence (PL) spectra of **Ir-Se** in CH_2Cl_2 solution.

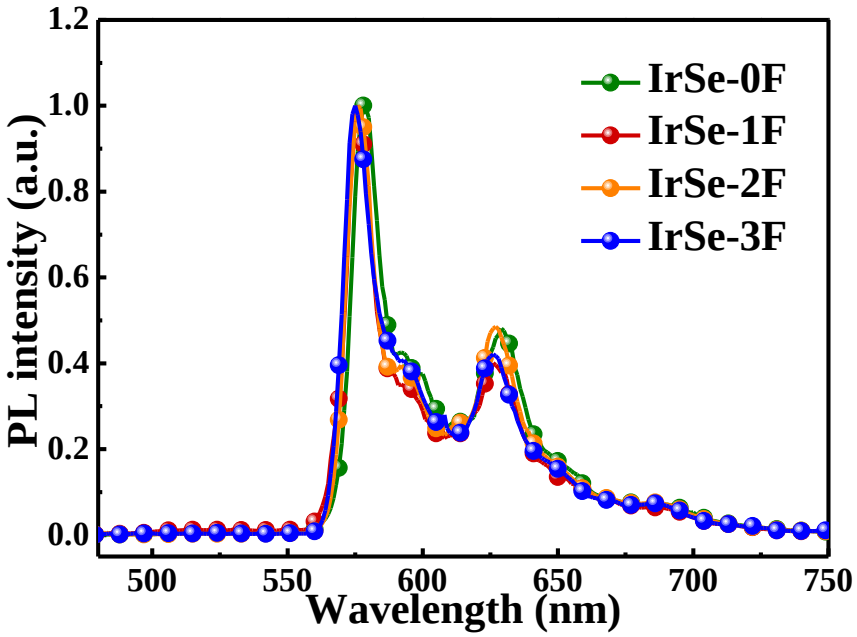

Figure S9. Photoluminescence (PL) spectra of the asymmetric heteroleptic Ir(III) complexes in CH_2Cl_2 solution recorded at 77 K.

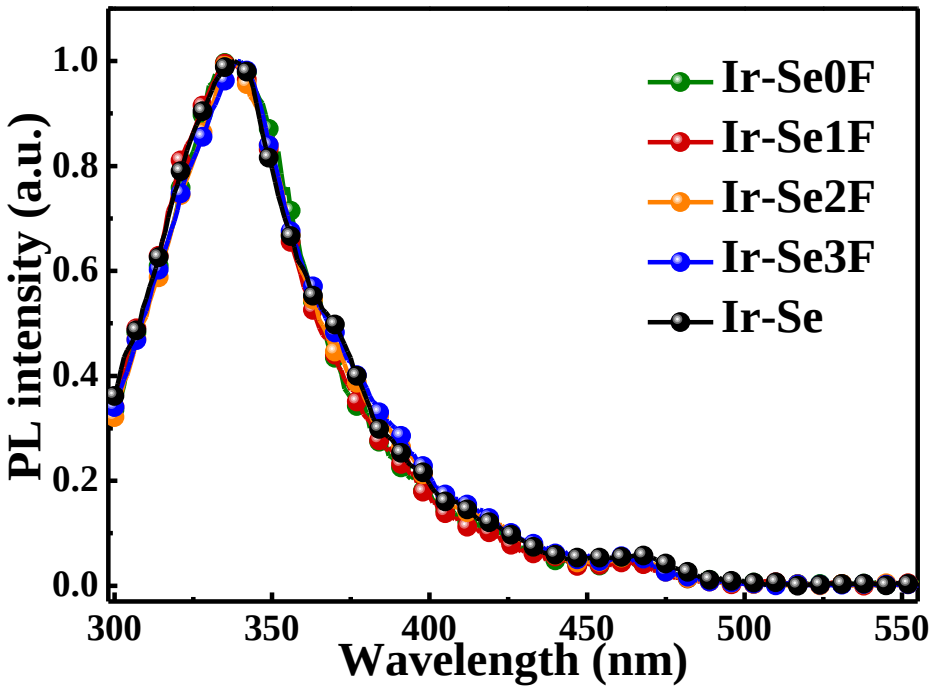

Figure S10. Excitation spectra of the asymmetric heteroleptic Ir(III) complexes and their parent complex **Ir-Se** (10^{-5} M) in CH_2Cl_2 solution at 293 K.

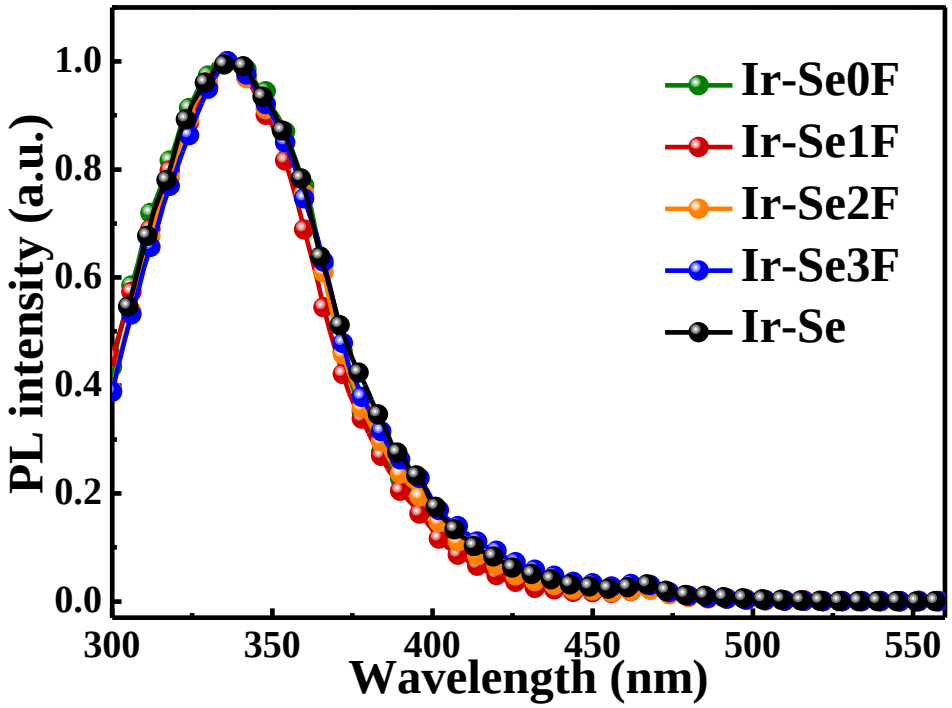

Figure S11. Excitation spectra of the asymmetric heteroleptic Ir(III) complexes and their parent complex **Ir-Se** doped into CBP films (8 wt%) at 293 K.

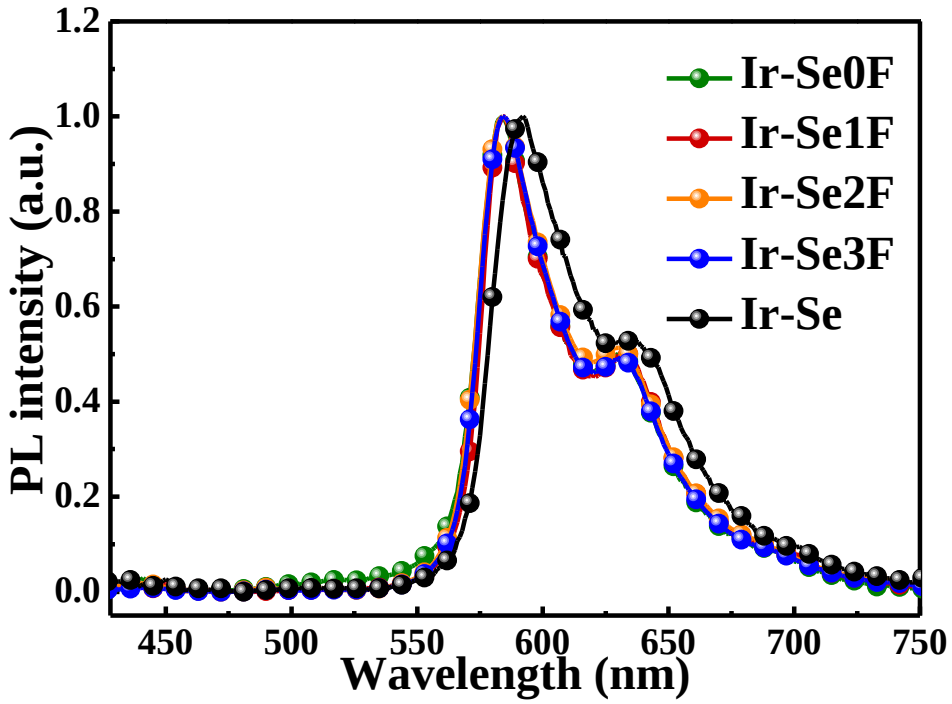

Figure S12. Photoluminescence (PL) spectra of the asymmetric heteroleptic Ir(III) complexes and their parent complex **Ir-Se** doped into CBP films (8 wt%) at 293 K.

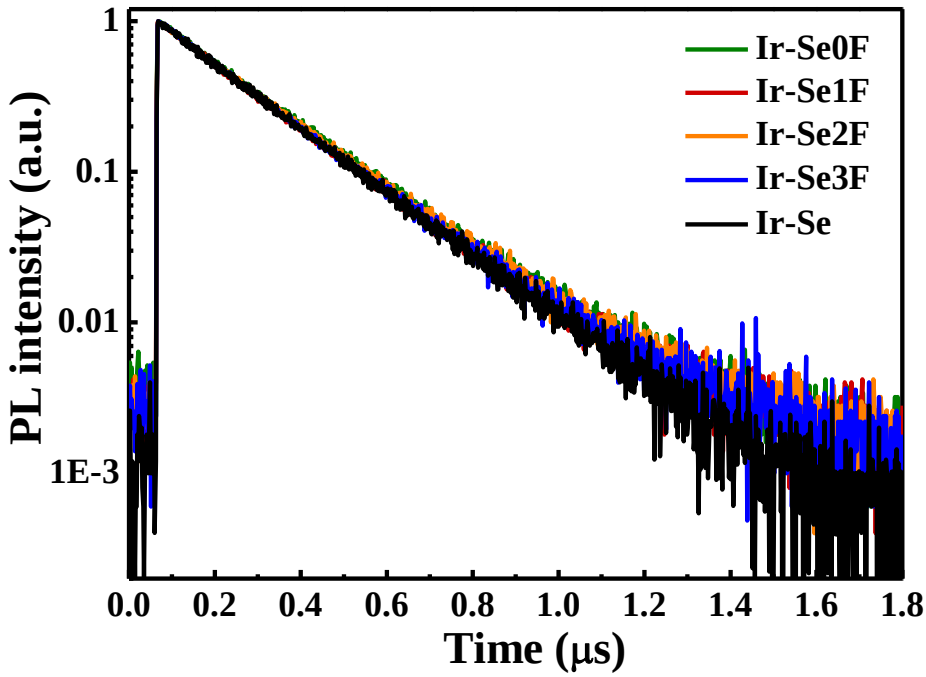

Figure S13. Transient photoluminescence (PL) spectra of the asymmetric heteroleptic Ir(III) complexes and their parent complex **Ir-Se** in CH_2Cl_2 (10^{-5} M) under aerated condition at 293 K.

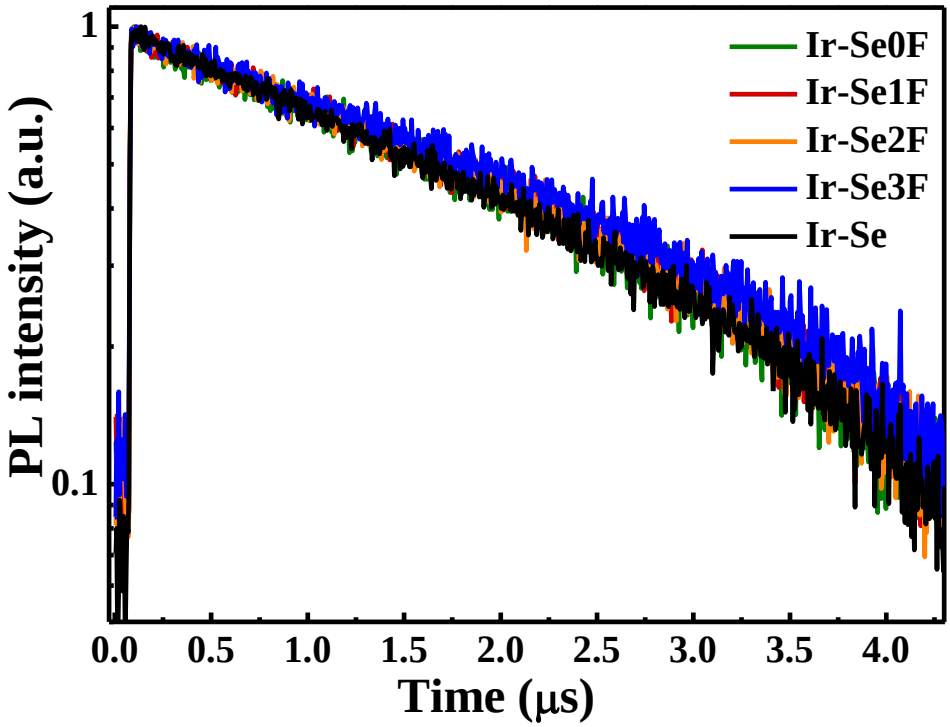

Figure S14. Transient photoluminescence (PL) spectra of the asymmetric heteroleptic Ir(III) complexes and their parent complex **Ir-Se** in CH_2Cl_2 (10^{-5} M) solution under degassed condition at 293 K.

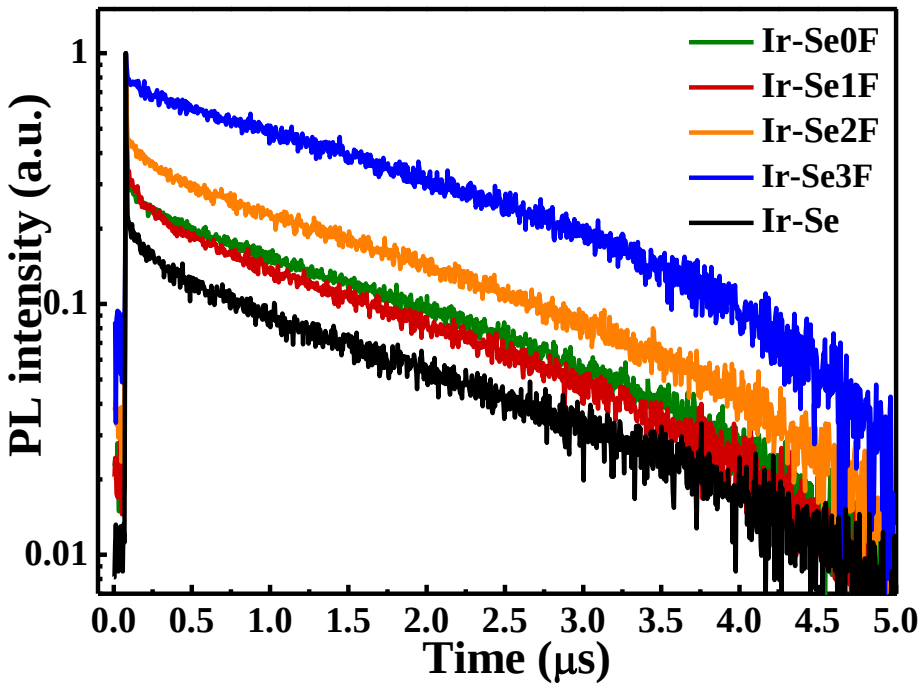

Figure S15. Transient photoluminescence (PL) spectra of the asymmetric heteroleptic Ir(III) complexes and their parent complex **Ir-Se** doped into CBP films (8 wt%) at 293 K.

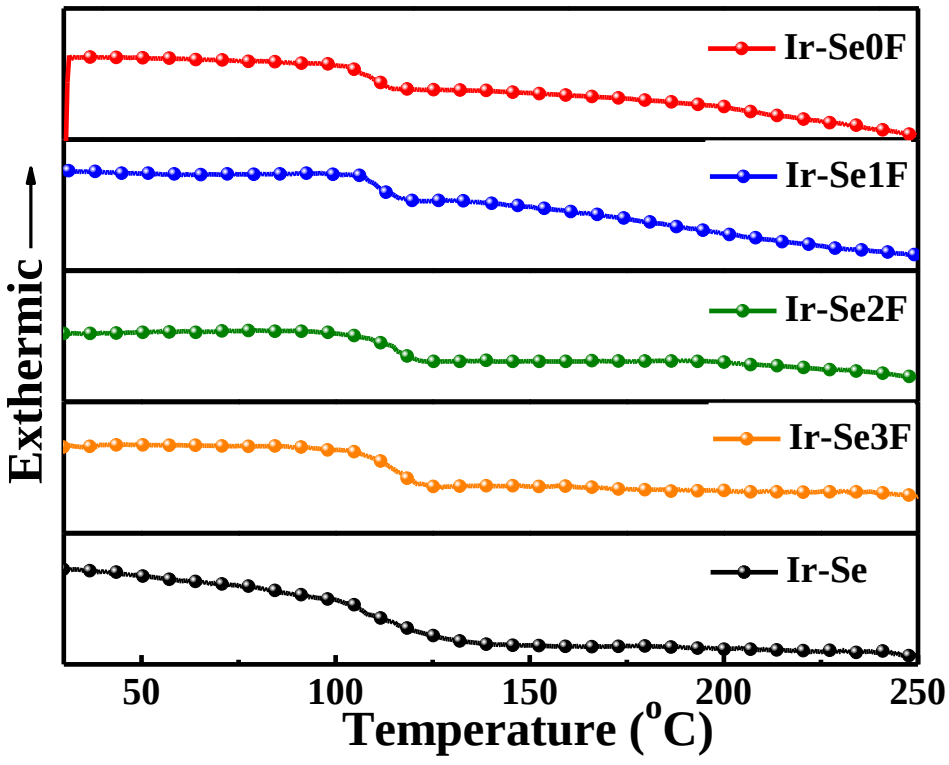

Figure S16. DSC traces of the asymmetric heteroleptic Ir(III) complexes and their parent complex **Ir-Se**.

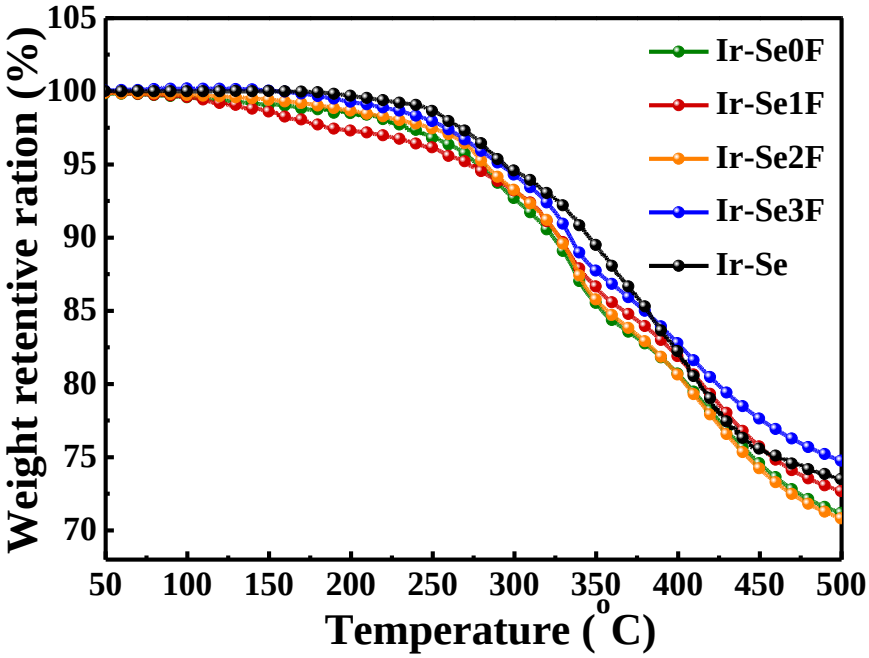

Figure S17. TGA traces of the asymmetric heteroleptic Ir(III) complexes and their parent complex **Ir-Se**.

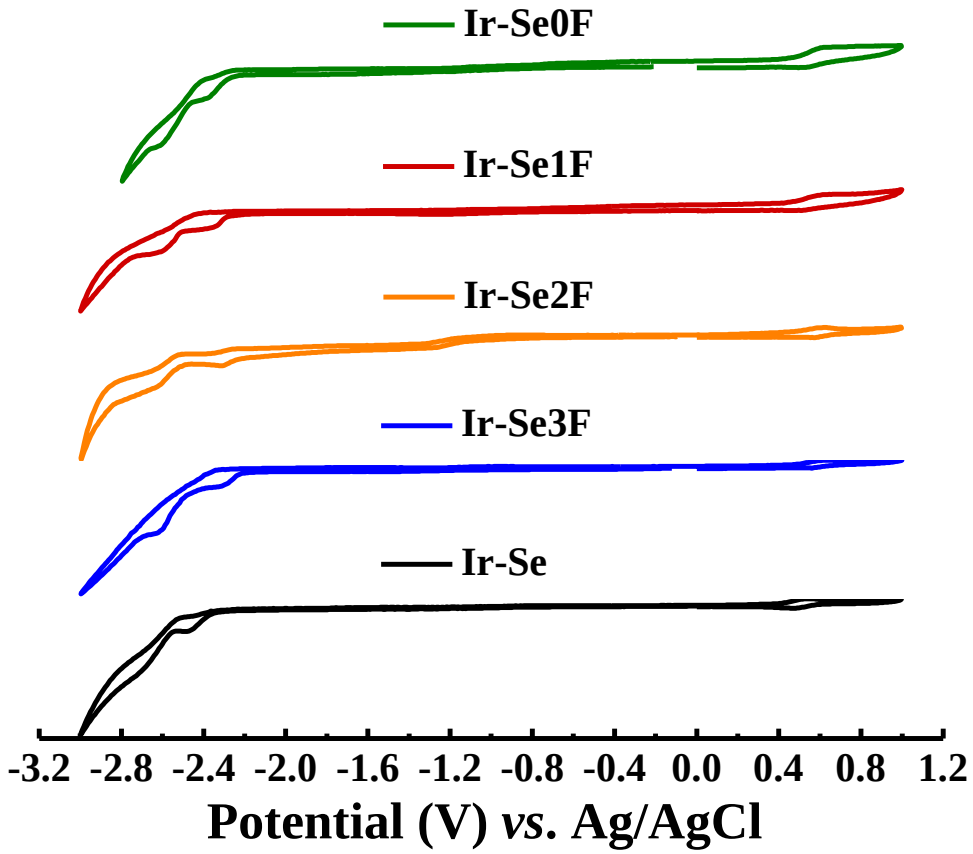

Figure S18. Cyclic voltammetry (CV) traces of the asymmetric heteroleptic Ir(III) complexes and their parent complex **Ir-Se**.

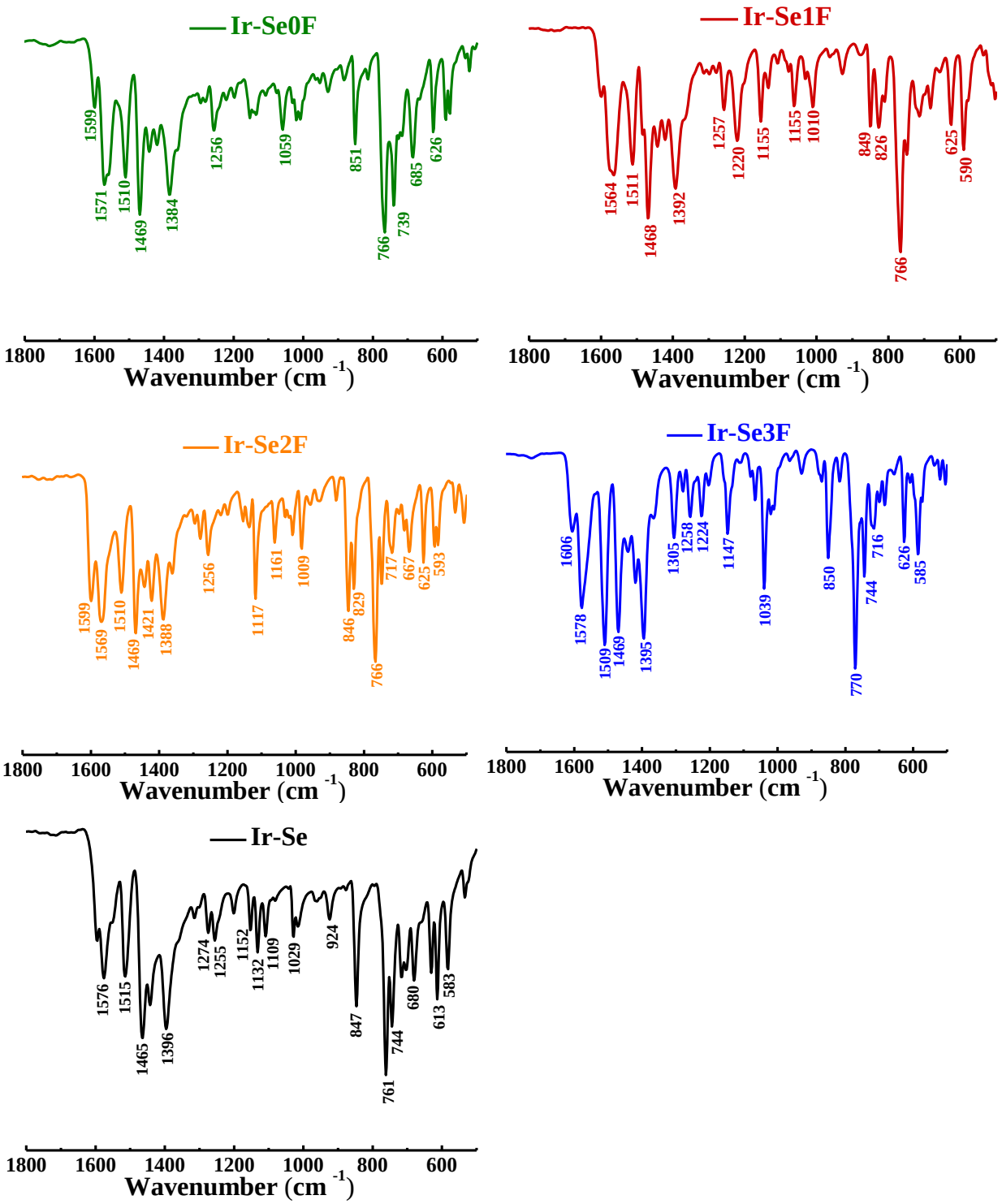

Figure S19. Infrared (IR) absorption spectra of the asymmetric heteroleptic Ir(III) complexes and their parent complex **Ir-Se**.

OLED Fabrication and Measurements. The pre-cleaned ITO glass substrates were dealt with ozone for 20 min before the PEDOT: PSS was spin-coated onto the surface of ITO glass to form a 45 nm-thick hole injection layer. After being cured at 120 ^{o}C for 30 min in the air, the emitting layer (40 nm) was obtained by spin-coating a chloroform solution of each asymmetric *bis*-heteroleptic Ir(III) complexes and 4,4'-*N*,*N*'-dicarbazole-biphenyl (CBP) at various concentration. The obtained ITO chip was dried in a vacuum oven at 50 ^{o}C for 20 min and transferred to the deposition system for organic and metal deposition. TPBi (1,3,5-*tris*-(*N*-(phenyl)-benzimidazole)-benzene) (45 nm), LiF (1 nm) and Al cathode (100 nm) were successively evaporated at a base pressure less than 10^{-6} Torr. The EL spectra and CIE coordinates were measured with a PR650 spectra colorimeter. The *J*–*V*–*L* curves of the devices were recorded by a Keithley 2400/2000 source meter and the luminance was measured using a PR650 SpectraScan spectrometer. All the experiments and measurements were carried out under ambient conditions.

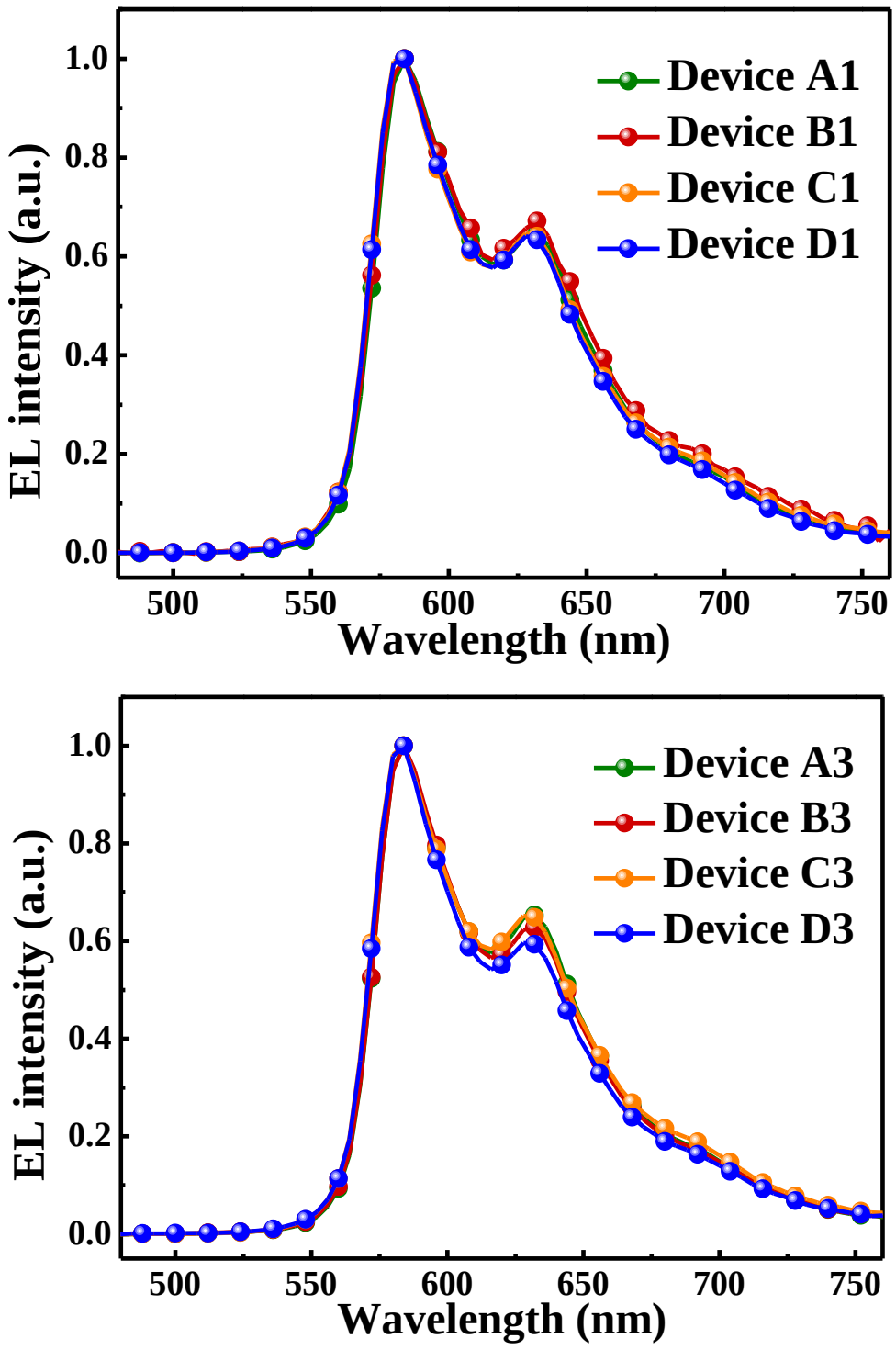

Figure S20. EL spectra for the devices except the optimized ones at *ca.* 10 V.

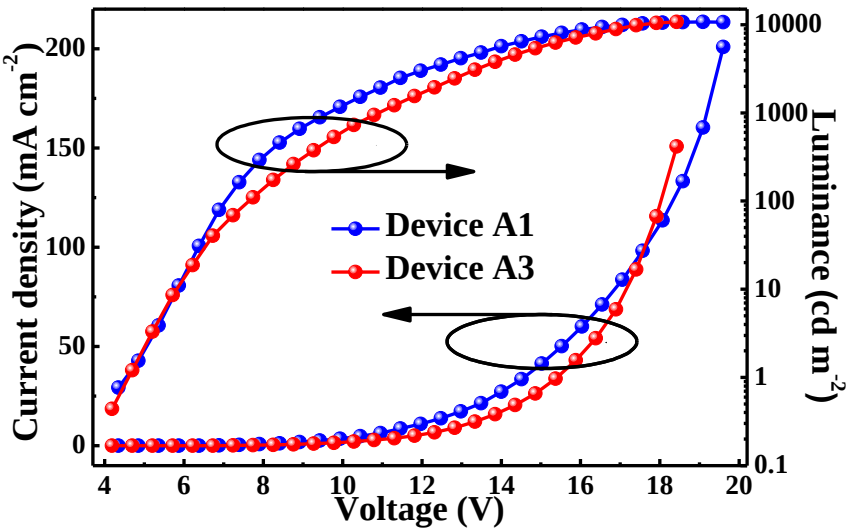
Current density (mA cm-2)
Luminance (cd m-2)
Voltage (V)
Device A1
Device A3

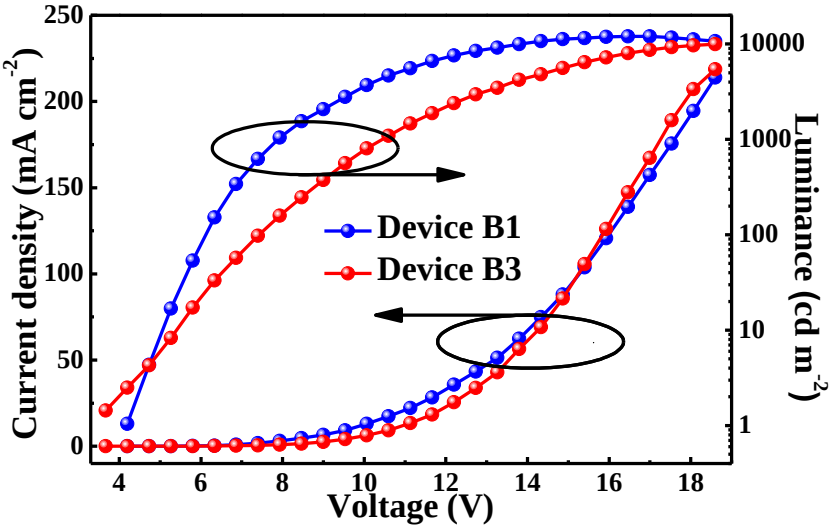
Current density (mA cm-2)
Luminance (cd m-2)
Voltage (V)
Device B1
Device B3

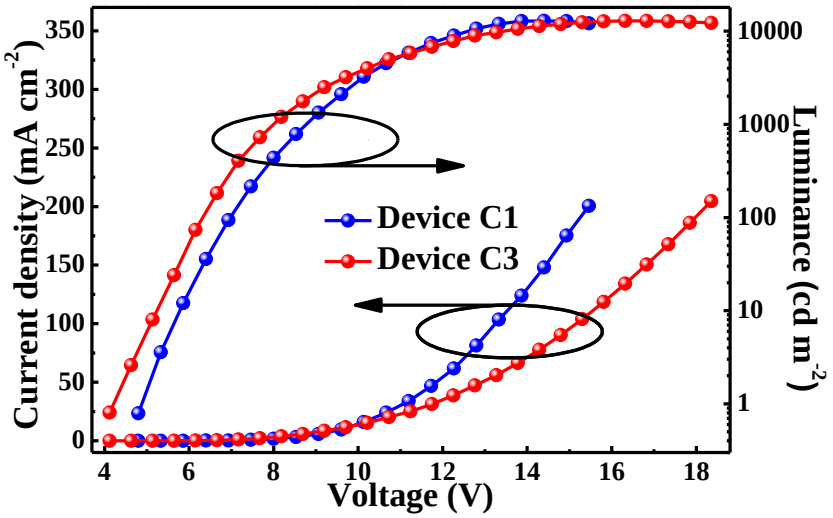
Current density (mA cm-2)
Luminance (cd m-2)
Voltage (V)
Device C1
Device C3

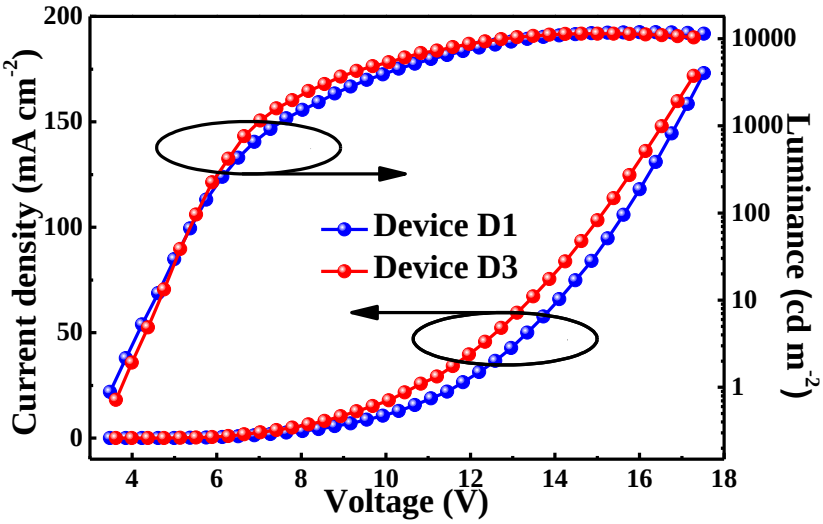

Figure S21. Current–density–voltage–luminance (*J–V–L*) curves for the devices except the optimized ones.

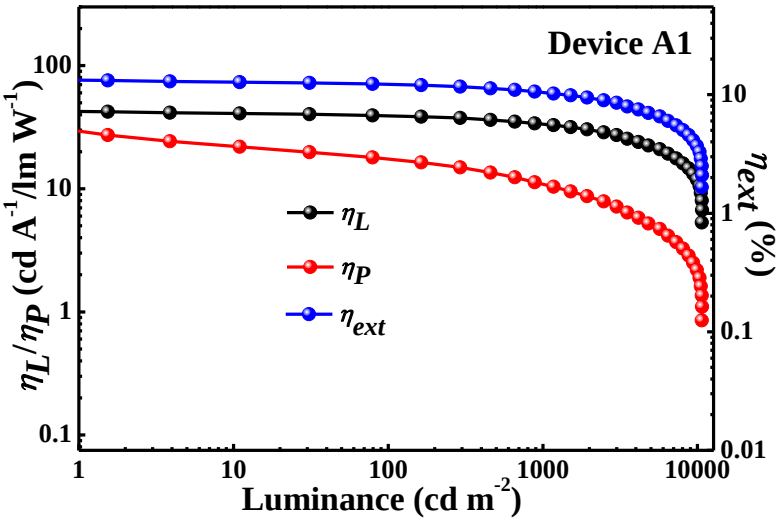

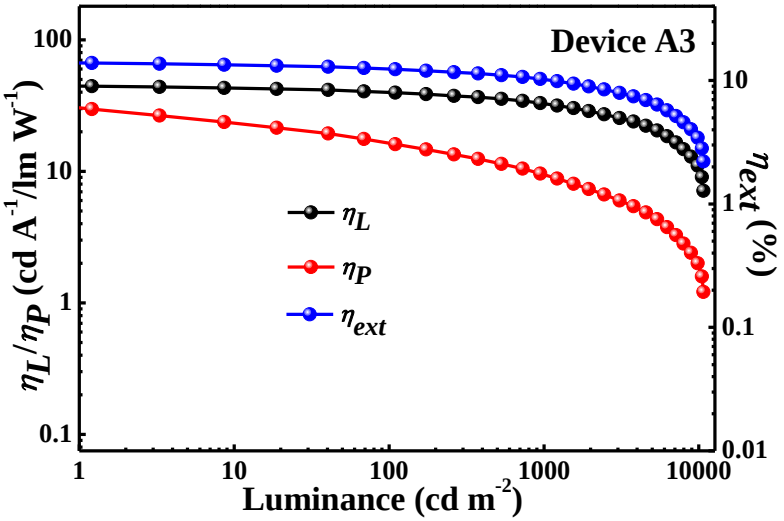

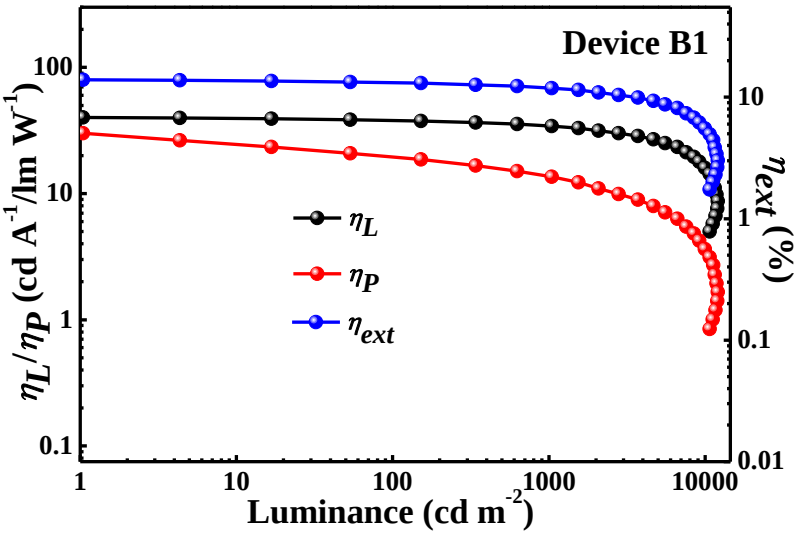
Device B1
η_L/η_P (cd A^{-1}/lm W^{-1})
η_{ext} (%)
Luminance (cd m^{-2})
η_L
η_P
η_{ext}
100
10
1
0.1
10
1
0.1
0.01
1
10
100
1000
10000

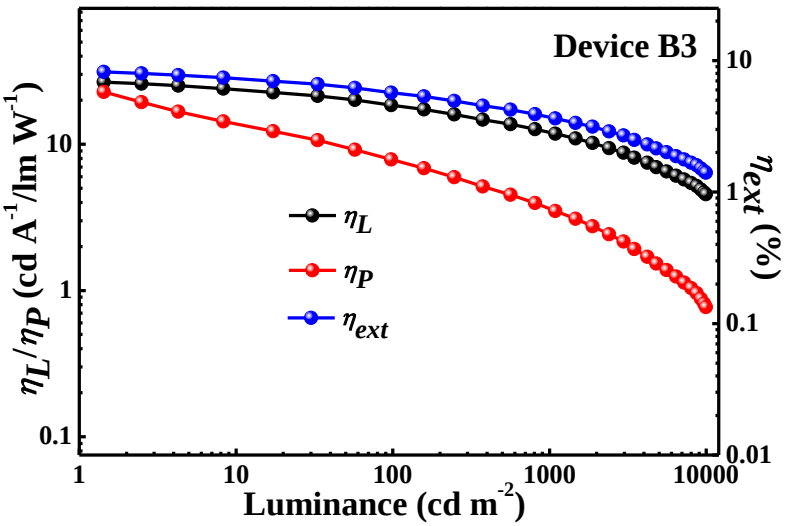
Device B3
η_L/η_P (cd A^{-1}/lm W^{-1})
η_{ext} (%)
Luminance (cd m^{-2})
η_L
η_P
η_{ext}
10
1
0.1
10
1
0.1
0.01
1
10
100
1000
10000

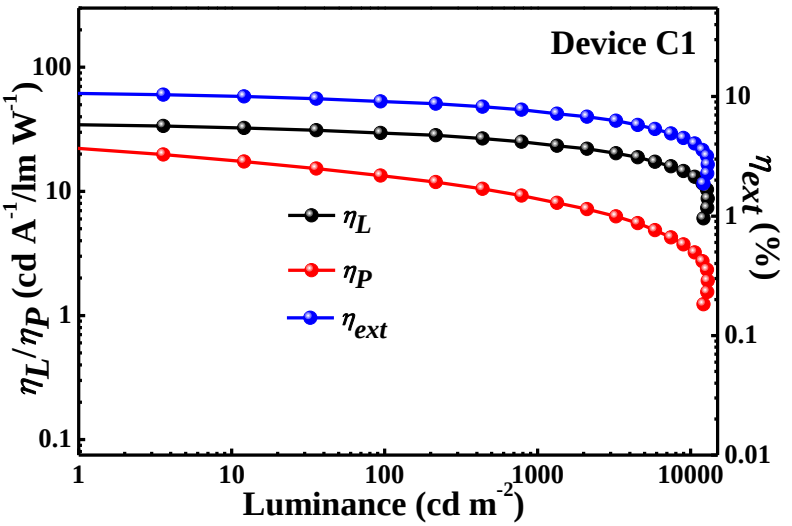
Device C1
η_L/η_P (cd A^{-1}/lm W^{-1})
η_{ext} (%)
Luminance (cd m^{-2})
η_L
η_P
η_{ext}
100
10
1
0.1
10
1
0.1
0.01
1
10
100
1000
10000

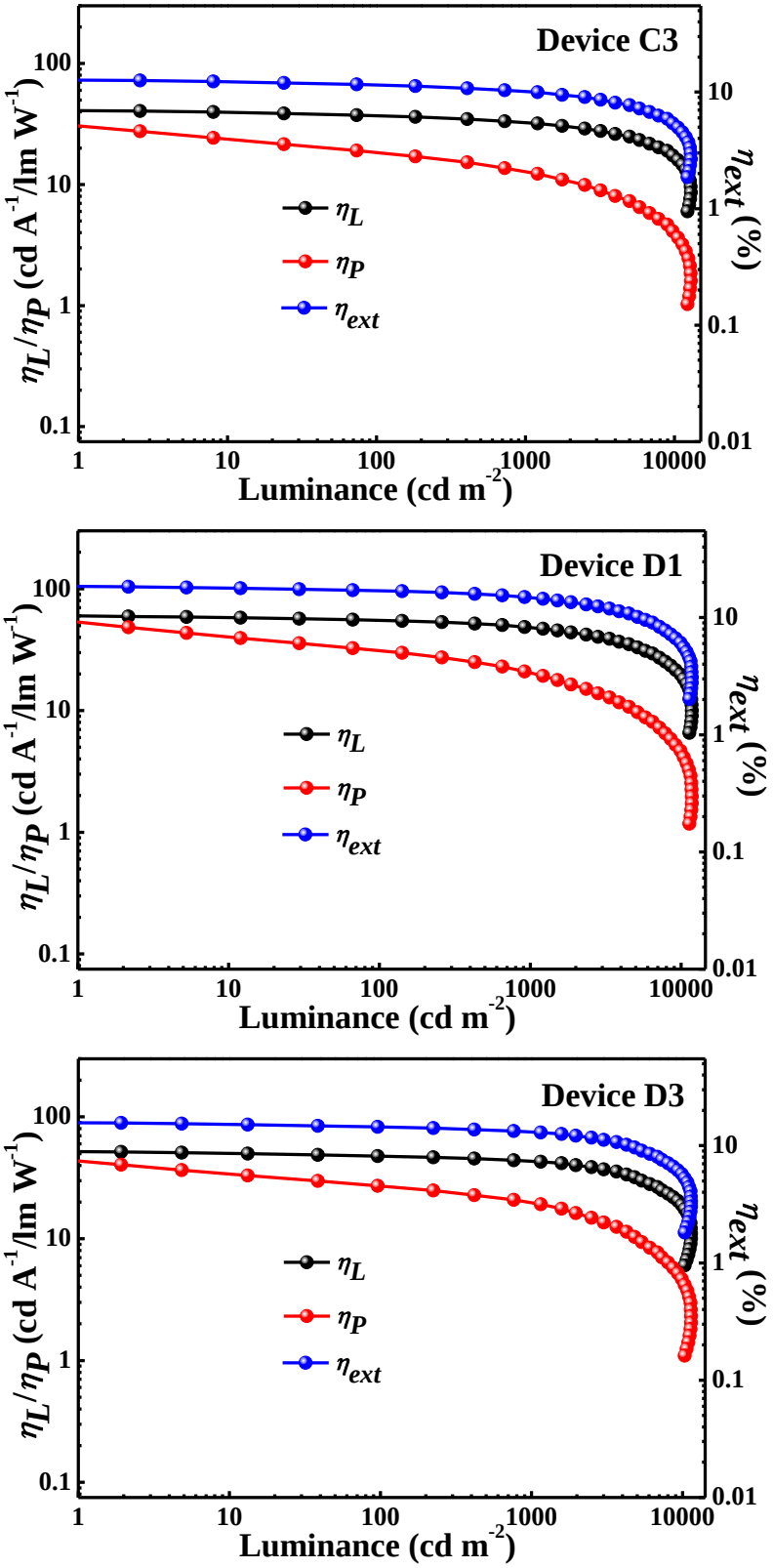

Figure S22. Relationship between EL efficiencies and luminance for the devices except the optimized ones.

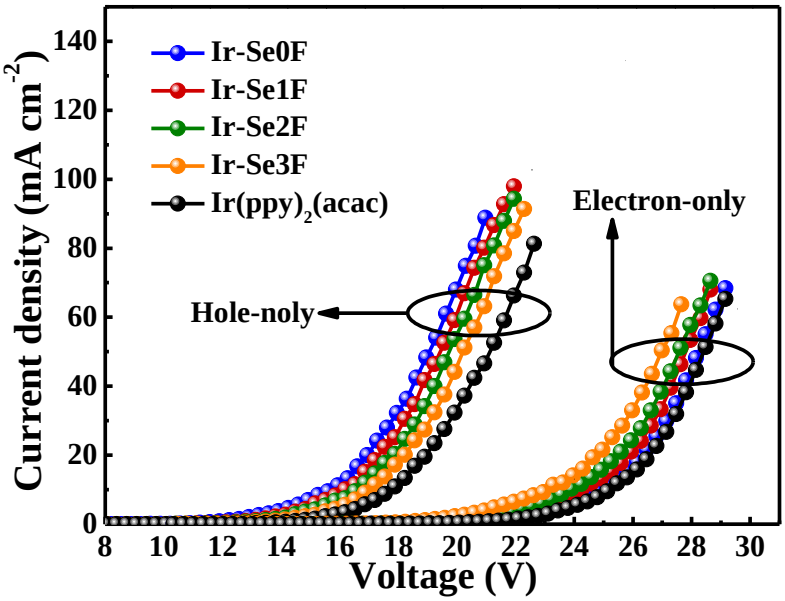

Figure S23. Current density–voltage (*J*–*V*) curves for single carrier devices with 8 wt% doped CBP films using the asymmetric heteroleptic Ir(III) complexes and **Ir(ppy)$_2$(acac)** as active layer. Hole-only device: ITO/MoO_3 (3nm)/PEDOT: PSS (20 nm)/active layer (50 nm)/NPB (30nm)/MoO_3 (3 nm)/Al (100 nm); electron-only device: ITO/LiF (3 nm)/active layer (50 nm)/LiF (3 nm)/Al (100 nm).